Commun. Comput. Phys.
doi: 10.4208/cicp.OA-2015-0005

Vol. **20**, No. 5, pp. 1283-1312
November 2016

Quadrature Weights on Tensor-Product Nodes for Accurate Integration of Hypersingular Functions over Some Simple 3-D Geometric Shapes

Brian Zinser[1], Wei Cai[1,*] and Duan Chen[1]

[1] *Department of Mathematics and Statistics, University of North Carolina at Charlotte, Charlotte, NC 28223, USA.*

Received 30 October 2015; Accepted (in revised version) 26 May 2016

Abstract. In this paper, we present accurate and economic integration quadratures for hypersingular functions over three simple geometric shapes in $\mathbb{R}^3$ (spheres, cubes, and cylinders). The quadrature nodes are made of the tensor-product of 1-D Gauss nodes on $[-1,1]$ for non-periodic variables or uniform nodes on $[0,2\pi]$ or $[0,\pi]$ for periodic ones. The quadrature weights are converted from a brute-force integration of the hypersingular function through interpolating the smooth component of the integrand. Numerical results are presented to validate the accuracy and efficiency of computing hypersingular integrals, as in the computations of Cauchy principal values, with a minimum number of quadrature nodes. The pre-calculated quadrature tables can be then readily used to implement Nyström collocation methods of hypersingular volume integral equations such as the one for Maxwell equations.

AMS subject classifications: 31B05, 92C05, 65Z05

Key words: Hypersingular integral, Cauchy principal value, tensor-product quadratures.

1 Introduction

The computation of hypersingular integrals associated with Cauchy principal values (CPVs) is the most time consuming and challenging task in solving integral equations for many mathematical physics equations, for example, Maxwell equations, elasticity equations, etc. The CPV is defined by the integration of the singular function by first excluding a small volume around the singularity, then letting the size of the exclusion volume shrink to zero to produce the CPV. Namely, the CPV is defined as

$$\text{p.v.}\int_\Omega \frac{f(\mathbf{r})}{|\mathbf{r}-\mathbf{r}'|^k}d\mathbf{r} = \lim_{\delta\to 0}\int_{\Omega\setminus V_\delta(\mathbf{r}')}\frac{f(\mathbf{r})}{|\mathbf{r}-\mathbf{r}'|^k}d\mathbf{r}, \tag{1.1}$$

*Corresponding author. *Email addresses:* bzinser@sandia.gov (B. Zinser), wcai@uncc.edu (W. Cai), duan.chen@uncc.edu (D. Chen)

where Ω is a bounded domain in R^3 assumed to be a cube, rectangular prism, cylinder, or sphere in this paper and $V_\delta(\mathbf{r}')$ is an exclusion volume centered at $\mathbf{r}'$ of spherical shape of radius δ.

The objective of this paper is to develop an accurate and efficient quadrature formula to compute the integral over $\Omega\backslash V_\delta(\mathbf{r}')$ in (1.1). For any fixed $\delta>0$, the integral over domain $\Omega\backslash V_\delta(\mathbf{r}')$ can be calculated by a naive brute-force approach to a given accuracy if a large number of sample points are used. Fortunately, the function $f(\mathbf{r})$ in the numerator, which can take a general form in the integral equation method, is often smooth; therefore, $f(\mathbf{r})$ can be well represented through an interpolation of its values on the three-dimensional tensor product of 1-D Gauss quadrature or midpoint nodes. Using this simple fact, any brute-force integration quadrature involving a large number of values of $f(\mathbf{r})$ can be converted into an equivalent quadrature formula using only values at the small number of nodes of a tensor-product form in Ω. Moreover, the new weights on the tensor-product nodes can be pre-computed and tabulated to be used for a general function $f(\mathbf{r})$. This will be the approach in this paper, and the resulting weights have been used to calculate the matrix entries for a discretized Nyström volume integral equation for Maxwell equations in [1] where the issue of CPV limit is also addressed. There are other approaches in computing the CPV in (1.1), including direct evaluations of hypersingular integrals [2].

The rest of this paper will be organized as follows. In Section 2, we will describe the interpolation approach for constructing a quadrature formula for singular integrations over the domain $\Omega\backslash V_\delta(\mathbf{r}')$ on tensor-product nodes. In Sections 3 through 5, we present specific implementations of interpolated quadrature when Ω is a cube, cylinder, and sphere, respectively. In Section 6, we provide an outline of the resulting algorithm that is implemented in computer code. In Section 7, numerical tests are included for each domain. In the appendix, quadrature weights over some tensor-product nodes are given for singular integrals over each domain.

2 Quadrature formula over tensor-product nodes

Consider a hypersingular integrand formed by the product of some smooth function $f(\mathbf{r})$ with a singular kernel $1/|\mathbf{r}-\mathbf{r}'|^k$ over a domain Ω, where the singularity is at $\mathbf{r}'\in\Omega$ and k can be 1, 2, or 3, i.e.,

$$\int_{\Omega\backslash V_\delta(\mathbf{r}')}\frac{f(\mathbf{r})}{|\mathbf{r}-\mathbf{r}'|^k}d\mathbf{r}. \tag{2.1}$$

First, assume we have an N point quadrature rule that uses points $\hat{\mathbf{r}}_i$ and weights $\hat{w}_i$,

$$\int_{\Omega\backslash V_\delta(\mathbf{r}')}\frac{f(\mathbf{r})}{|\mathbf{r}-\mathbf{r}'|^k}d\mathbf{r}\approx\sum_{i=1}^{N}\frac{f(\hat{\mathbf{r}}_i)}{|\hat{\mathbf{r}}_i-\mathbf{r}'|^k}\hat{w}_i. \tag{2.2}$$

As the function $f(\mathbf{r})$ is generally smooth, it can be well approximated through an interpolation of its values over a small number of tensor-product nodes $\{\mathbf{r}_i\}|_{i=1}^M$. Letting

$\phi_j(\mathbf{r})$ denote a set of M basis functions that satisfy the Kronecker delta property $\phi_j(\mathbf{r}_i) = \delta_{i,j}$, we have the following approximation:

$$f(\mathbf{r}) \approx \sum_{j=1}^{M} f(\mathbf{r}_j)\phi_j(\mathbf{r}). \tag{2.3}$$

Then, we can manipulate (2.1) as follows:

$$\begin{aligned}\int_{\Omega\setminus V_\delta(\mathbf{r}')} \frac{f(\mathbf{r})}{|\mathbf{r}-\mathbf{r}'|^k} d\mathbf{r} &\approx \sum_{i=1}^{N} \frac{f(\hat{\mathbf{r}}_i)}{|\hat{\mathbf{r}}_i-\mathbf{r}'|^k}\hat{w}_i \approx \sum_{i=1}^{N}\left(\sum_{j=1}^{M}\frac{f(\mathbf{r}_j)\phi_j(\hat{\mathbf{r}}_i)}{|\hat{\mathbf{r}}_i-\mathbf{r}'|^k}\hat{w}_i\right)\\ &= \sum_{j=1}^{M} f(\mathbf{r}_j)\left(\sum_{i=1}^{N}\frac{\phi_j(\hat{\mathbf{r}}_i)}{|\hat{\mathbf{r}}_i-\mathbf{r}'|^k}\hat{w}_i\right).\end{aligned} \tag{2.4}$$

Therefore, we obtain an M-point quadrature formula over the tensor-product nodes as follows:

$$\int_{\Omega\setminus V_\delta(\mathbf{r}')} \frac{f(\mathbf{r})}{|\mathbf{r}-\mathbf{r}'|^k} d\mathbf{r} \approx \sum_{j=1}^{M} f(\mathbf{r}_j) w_{j,k}, \tag{2.5}$$

where the quadrature weights are given by

$$w_{j,k} = \sum_{i=1}^{N} \frac{\phi_j(\hat{\mathbf{r}}_i)}{|\hat{\mathbf{r}}_i-\mathbf{r}'|^k}\hat{w}_i. \tag{2.6}$$

It can be easily seen that the weight is a quadrature approximation for the following integral

$$w_{j,k} \simeq \int_{\Omega\setminus V_\delta(\mathbf{r}')} \frac{\phi_j(\mathbf{r})}{|\mathbf{r}-\mathbf{r}'|^k} d\mathbf{r}. \tag{2.7}$$

It should be noted that $w_{j,k}$ can be precalculated. Moreover, in our implementation of the quadrature rule in (2.2), we use spherical coordinates in a region around $\mathbf{r}'$; $\hat{w}_i$ then contains the Jacobian $|\hat{\mathbf{r}}_i-\mathbf{r}'|^2$ when $\hat{\mathbf{r}}_i$ is near $\mathbf{r}'$, which reduces the order of the singularity. When k is less than 3, the limit in (1.1) can be evaluated once this Jacobian is applied and the size δ of the exclusion volume $V_\delta(\mathbf{r}')$ can be taken to be zero. As M is usually small ($M << N$) in the interpolation formula (2.3) for $f(\mathbf{r})$, the new quadrature formula (2.5) will be fast, using only a small number of samples. The error committed in (2.5) is twofold: error occurs when we use the initial brute-force quadrature rule to approximate the integral in (2.2), which can be controlled by increasing the number N, and when we approximate $f(\mathbf{r})$ by using basis functions $\phi_j(\mathbf{r})$ and the samples $f(\mathbf{r}_j)$. However, if the basis $\phi_j(\mathbf{r})$ is the same one used to approximate the solution of, for example, a volume integral equation by a Nyström collocation method, then the error due to interpolating $f(\mathbf{r})$ will be of the same order as expected in the underlying Nyström VIE method.

Finally, it is desirable to make a reference domain $\Omega\backslash V_\delta(\mathbf{r}')$ for calculating the integral over some different sized domain $\hat{\Omega}$ where the mapping from $\Omega\backslash V_\delta(\mathbf{r}')$ to $\hat{\Omega}$ is given by $\gamma(\mathbf{r})=a\mathbf{r}$ for some a. Then the Jacobian is given by $J_\gamma=a^{3-k}$ so that (2.5) becomes

$$\int_{\hat{\Omega}}\frac{f(\mathbf{r})}{|\mathbf{r}-\mathbf{r}'|^k}d\mathbf{r}\approx\sum_{j=1}^{M}f(\gamma(\mathbf{r}_j))J_\gamma w_{j,k}. \tag{2.8}$$

This is because the sum over i in (2.4) is calculated on the reference element. If an exclusion $V_\delta(\mathbf{r}')$ is present, care should be taken to be aware of any deformation caused by the mapping, if any.

3 M-point tensor-product quadratures for a cube or rectangular prism

3.1 Quadrature rule when the singularity $\mathbf{r}'$ is at the center of the cube

In the derivation of (2.5) for a cube, we take $\Omega=[-1,1]^3$. We proceed by subdividing Ω so that we have six pyramids P_i, $i=1,2,\cdots,6$, each using a different side of the cube as its base and $\mathbf{r}'=(0,0,0)$ for its pinnacle. Since we wish to use spherical coordinates (ρ,φ,θ) to reduce the singularity of the kernel, we rewrite (2.7) as

$$\begin{aligned}\int_{\Omega\backslash V_\delta(\mathbf{r}')}\frac{\phi_j(\mathbf{r})}{|\mathbf{r}-\mathbf{r}'|^k}d\mathbf{r}&=\sum_{i=1}^{6}\int_{P_i\backslash V_\delta(\mathbf{r}')}\frac{\phi_j(\mathbf{r})}{|\mathbf{r}-\mathbf{r}'|^k}d\mathbf{r}\\&=\sum_{i=1}^{6}\int_{\rho_{i,\min}}^{\rho_{i,\max}}\int_{\theta_{i,\min}}^{\theta_{i,\max}}\int_{\varphi_{i,\min}}^{\varphi_{i,\max}}\frac{\phi_j(\mathbf{r})}{|\mathbf{r}-\mathbf{r}'|^k}\rho^2\sin(\theta)d\varphi d\theta d\rho.\end{aligned} \tag{3.1}$$

For the pyramid with a base at $x=1$, the limits of integration are

$$\begin{aligned}&\varphi_{\min}=-\frac{\pi}{4},\quad \theta_{\min}=\frac{\pi}{2}-\tan^{-1}(\cos(\varphi)),\quad \rho_{\min}=\delta,\\&\varphi_{\max}=\frac{\pi}{4},\quad \theta_{\max}=\frac{\pi}{2}+\tan^{-1}(\cos(\varphi)),\quad \rho_{\max}=\frac{1}{\cos(\varphi)\sin(\theta)}.\end{aligned} \tag{3.2}$$

We now define several mappings from $[0,1]$, where we have n one-dimensional Gauss points and weights (t_ℓ,w_ℓ^t), to the variables of integration in (3.2).

Working with the pyramid whose base satisfies $x=1$, we map a Gauss point-weight pair (t_k,w_k^t) to its corresponding azimuthal angle and weight (φ_k,w_k^φ) by

$$\varphi_k=\tfrac{\pi}{4}(t_k-1),\quad w_k^\varphi=w_k^t. \tag{3.3}$$

Next, for a fixed angle φ_k, we map a Gauss point-weight pair (t_j,w_j^t) to its corresponding angle of inclination and weight (θ_j,w_j^θ) by

$$\begin{aligned}&\theta_{j,k}=2\tan^{-1}(\cos(\varphi_k))t_j+\frac{\pi}{2}-\tan^{-1}(\cos(\varphi_k)),\\&w_{j,k}^\varphi=2\tan^{-1}(\cos(\varphi_k))w_j^t.\end{aligned} \tag{3.4}$$

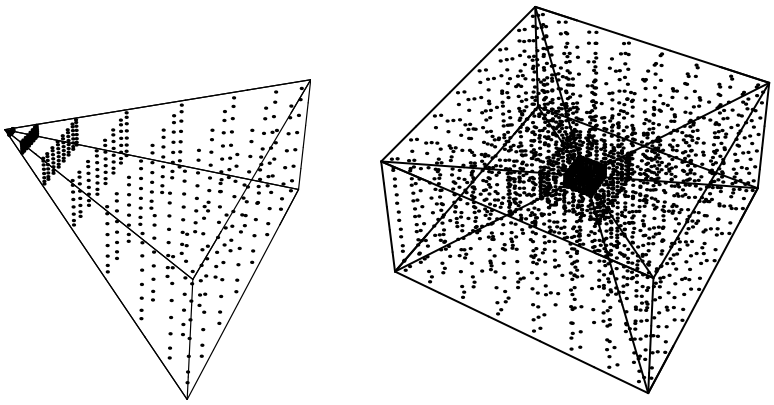

Figure 1: Quadrature points on the pyramid with base satisfying $x=1$ (left) and on the cube $[-1,1]^3$ (right).

For fixed angles φ_k and θ_j, we map a Gauss point-weight pair (t_i, w_i^t) to its corresponding radius and weight $(\rho_i, w_{i,j,k}^{\rho})$ by

$$\begin{aligned} \rho_{i,j,k} &= \left(\frac{1}{\cos(\varphi_k)\sin(\theta_{j,k})} - \rho_{\min}\right) t_i + \rho_{\min}, \\ w_{i,j,k}^{\rho} &= \left(\frac{1}{\cos(\varphi_k)\sin(\theta_{j,k})} - \rho_{\min}\right) w_i^t, \end{aligned} \tag{3.5}$$

where $\rho_{\min}=\delta$ if a sphere around the singularity is excluded. Otherwise, $\rho_{\min}=0$. Matching indices, we now have a set of n^3 points and weights on the pyramid given by

$$\{(\rho_{i,j,k}, \theta_{j,k}, \varphi_k) : 1 \le i,j,k \le n\},\ \{w_{i,j,k}^{\rho} w_{j,k}^{\theta} w_k^{\varphi} : 1 \le i,j,k \le n\}. \tag{3.6}$$

Finally, the points are converted to Cartesian coordinates. The quadrature points on the remaining five pyramids can either be handled by the same method or can be calculated from these points and weights by a rotation. We take the latter approach. For $n=8$, the resulting quadrature points are plotted in Fig. 1. In total, there are $N=6n$ sample points in the cube on the right of Fig. 1. While the points are mostly symmetrical, the y-coordinates differ from the z-coordinates slightly in the pyramid on the left. If desired, a more symmetrical quadrature rule could be found without difficulty.

3.2 Quadrature rule when the singularity $\mathbf{r}'$ is not at the center of the cube or Ω is a rectangular prism

There are two straightforward approaches for the case when $\mathbf{r}'$ is not at the center of the cube. One way is to modify the formulas for finding the quadrature points on the pyramids so that the pyramids are deformed; in this case, each pyramid should be calculated independently instead of using a rotation as before. However, this will result in some

pyramids that are too flat to be integrated accurately if the singularity is located near the edge of the cube. As our primary goal is to compute the integral near the singularity accurately, we implement a second way where a subcube is made with the singularity at its center; the remaining regions of the parent cube $[-1,1]^3$ are subdivided and integrated using the cross-product of n_{reg} Gauss points and weights (t_ℓ, w_ℓ^t) defined on a reference cube $[0,1]^3$ by

$$\begin{aligned}&\{(t_i,t_j,t_k):1\le i,j,k\le n_{reg}\},\\&\{w_i^t w_j^t w_k^t:1\le i,j,k\le n_{reg}\}.\end{aligned}\tag{3.7}$$

We take the subcube with the singularity at its center to be the largest contained in the parent cube $[-1,1]^3$. In our implementation, this means that if the singularity is at the center of the parent cube, the subcube is identical to the parent cube. If the singularity is equidistant from three adjacent faces of the parent cube, it is in a corner and we calculate 7 additional nonsingular integrals. If the singularity is equidistant from two adjacent faces, it is near an edge and we calculate 11 additional integrals. Otherwise, we calculate 17 additional integrals so

$$N\le 6n^3+17n_{reg}^3.\tag{3.8}$$

Illustrations of these cases are shown in Fig. 2. The integral in (2.7) can be rewritten to include I nonsingular subregions R_i, $i=1,2,\cdots,I$, as

$$\begin{aligned}\int_{\Omega\setminus V_\delta(\mathbf{r}')}\frac{\phi_j(\mathbf{r})}{|\mathbf{r}-\mathbf{r}'|^k}d\mathbf{r}&=\sum_{i=1}^{6}\int_{P_i\setminus V_\delta(\mathbf{r}')}\frac{\phi_j(\mathbf{r})}{|\mathbf{r}-\mathbf{r}'|^k}d\mathbf{r}+\sum_{i=1}^{I}\int_{R_i}\frac{\phi_j(\mathbf{r})}{|\mathbf{r}-\mathbf{r}'|^k}d\mathbf{r}\\&=\sum_{i=1}^{6}\int_{\rho_{i,\min}}^{\rho_{i,\max}}\int_{\theta_{i,\min}}^{\theta_{i,\max}}\int_{\varphi_{i,\min}}^{\varphi_{i,\max}}\frac{\phi_j(\mathbf{r})}{|\mathbf{r}-\mathbf{r}'|^k}\rho^2\sin(\theta)d\varphi d\theta d\rho\\&+\sum_{i=1}^{I}\int_{x_{i,\min}}^{x_{i,\max}}\int_{y_{i,\min}}^{y_{i,\max}}\int_{z_{i,\min}}^{z_{i,\max}}\frac{\phi_j(\mathbf{r})}{|\mathbf{r}-\mathbf{r}'|^k}dzdydx,\end{aligned}\tag{3.9}$$

where the union of the regions P_i make up the singular subcube, requiring $\rho_{i,\max}$ to be scaled appropriately.

These additional subregions allow Ω to be a rectangular prism, if desired. None of the subregions should have a dimension that is significantly larger than one of its other dimensions; otherwise this could lead to an inaccurate approximation over the subregion. Our code provides the option to allow further subdivision in case this is an issue.

3.3 M-point tensor-product quadratures for a cube

To construct the quadrature weights defined in (2.6) for a set of tensor-product nodes corresponding to 1-D Gauss points on $[-1,1]$, we will first define the interpolation functions. We use the cross-product of Lagrange polynomials defined on $[-1,1]$ for interpolation. Thus, we use

$$\{(2t_i-1,2t_j-1,2t_k-1):1\le i,j,k\le m\}\tag{3.10}$$

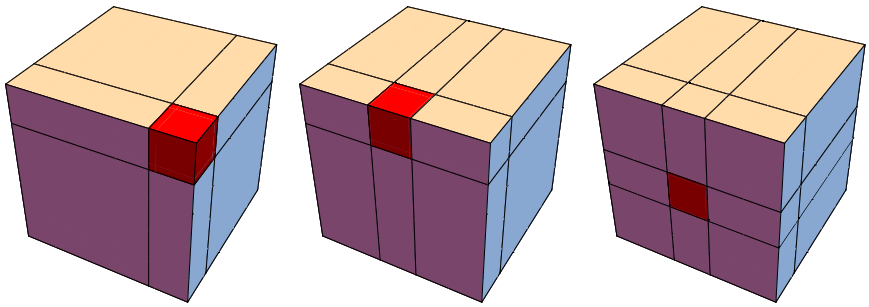

Figure 2: From left to right, the illustrations correspond to subdivisions when the singularity is in a corner, near an edge, and at the center of a face. The subcube with a singularity is red.

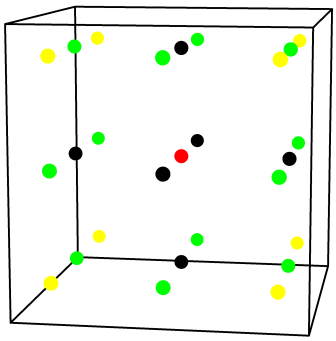

Figure 3: Interpolation points, colored to show rotationally symmetric points, on the cube when $m=3$ and $M=27$.

for our $M=m^3$ interpolation points $\mathbf{r}_j$ in $\mathbb{R}^3$, where t_ℓ are the m Gauss points defined on $[0,1]$. For the x-axis, the i^{th} Lagrange polynomial is given by

$$\ell_i^x(x)=\prod_{1\le p\le m, p\neq i}\frac{x-t_p}{t_i-t_p}. \tag{3.11}$$

The polynomials for y and z are similar. The resulting three-dimensional Lagrange polynomials are given by

$$L_{i,j,k}(\mathbf{r})=\ell_i^x(x)\ell_j^y(y)\ell_k^z(z). \tag{3.12}$$

Renaming and reindexing $L_{i,j,k}(\mathbf{r})$ as $\phi_j(\mathbf{r})$, we get a set of basis functions that satisfies (2.3). Then, we use our N-point quadrature rule over the cube to integrate the basis functions against the singular kernel as in (2.6). This produces the weights $w_{j,k}$. Finally, the integral over the cube $[-1,1]^3$ is given by (2.5). The degree of the one-dimensional basis functions can be set independently in case one dimension is much larger than another one, as is sometimes the case for a rectangular prism.

4 M-point tensor-product quadratures for a cylinder

4.1 Quadrature rule for a subcylinder centered at the singularity $\mathbf{r}'$

We begin with a cylinder of radius 1 whose bases satisfy $z=-1$ and $z=1$. For now, let the singularity $\mathbf{r}'=(0,0,0)$ be at the center of the cylinder. The cylinder can be subdivided into two cones C_1 and C_2 with the same bases as the cylinder and a third subregion C_3 that contains the sides of the cylinder. Using spherical coordinates (ρ,φ,θ) to reduce the singularity of the kernel, (2.7) becomes

$$\begin{aligned}&\int_{\Omega\setminus V_\delta(\mathbf{r}')}\frac{\phi_j(\mathbf{r})}{|\mathbf{r}-\mathbf{r}'|^k}d\mathbf{r}=\sum_{i=1}^{3}\int_{C_i\setminus V_\delta(\mathbf{r}')}\frac{\phi_j(\mathbf{r})}{|\mathbf{r}-\mathbf{r}'|^k}d\mathbf{r}\\&=\left[\int_\delta^{\frac{1}{\cos(\theta)}}\int_0^{\frac{\pi}{4}}+\int_\delta^{\frac{1}{\sin(\theta)}}\int_{\frac{\pi}{4}}^{\frac{3\pi}{4}}+\int_\delta^{-\frac{1}{\cos(\theta)}}\int_{\frac{3\pi}{4}}^{\pi}\right]\int_0^{2\pi}\frac{\phi_j(\mathbf{r})\rho^2\sin(\theta)}{|\mathbf{r}-\mathbf{r}'|^k}d\varphi d\theta d\rho.\end{aligned}\tag{4.1}$$

Let the n one-dimensional Gauss points and weights over $[0,1]$ be denoted by (t_ℓ,w_ℓ^t). For the azimuthal angle,

$$\varphi_k=2\pi\left(k+\frac{1}{2}\right)/n,\quad w_k^\varphi=2\pi k/n.\tag{4.2}$$

The angle of inclination is divided into three regions. For the cone with an apex at the singularity and the base at $z=1$,

$$\theta_j=\frac{\pi}{4}t_j,\quad w_j^\theta=\frac{\pi}{4}w_j^t.\tag{4.3}$$

For the cone with an apex at the singularity and the base at $z=-1$,

$$\theta_j=\frac{\pi}{4}t_j+\frac{3\pi}{4},\quad w_j^\theta=\frac{\pi}{4}w_j^t.\tag{4.4}$$

For the remaining region along the sides of the cylinder,

$$\theta_j=\frac{\pi}{2}t_j+\frac{\pi}{4},\ w_j^\theta=\frac{2\pi}{4}w_j^t.\tag{4.5}$$

Combining the n points for θ in each region, we use $3n$ points to integrate in the θ direction. Since ρ depends on θ, its formula changes depending on the region. For the upper cone, let $\rho_j^{\max}=1/\cos(\theta_j)$. For the lower cone, let $\rho_j^{\max}=-1/\cos(\theta_j)$. For the remaining side regions, let $\rho_j^{\max}=1/\sin(\theta_j)$. Then the points and weights for ρ are given by

$$\begin{aligned}\rho_{i,j}&=\left(\rho_j^{\max}-\rho_{\min}\right)t_i+\rho_{\min},\\w_{i,j}^\rho&=\left(\rho_j^{\max}-\rho_{\min}\right)w_i^t,\end{aligned}\tag{4.6}$$

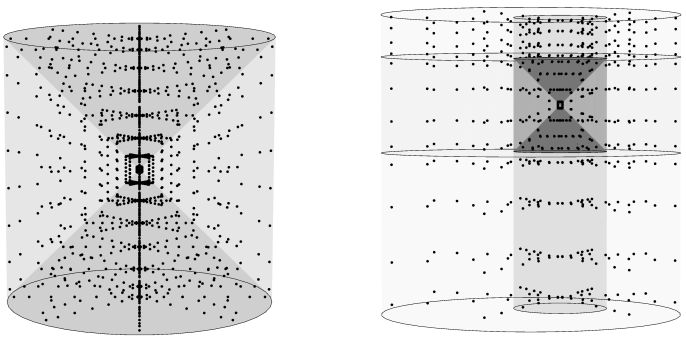

Figure 4: Quadrature points for the subcylinders. Left: The subcylinder with $\mathbf{r}'$ at its center when $n=8$; right: all subcylinders when $\mathbf{r}'=(0.2,0.3,0.4)$ when $n=n_{cyl}=n_w=4$.

where $\rho_{\min}=\delta$ if a sphere around the singularity is excluded. Otherwise, $\rho_{\min}=0$. Thus, this cylinder with the singularity at its center uses a total of $3n^3$ points, given by

$$\begin{aligned}&\{(\rho_{i,j},\theta_j,\varphi_k):1\le i,k\le n,1\le j\le 3n\},\\&\{w^{\rho}_{i,j}w^{\theta}_j w^{\varphi}_k:1\le i,k\le n,1\le j\le 3n\},\end{aligned}\tag{4.7}$$

which can be seen on the left of Fig. 4.

4.2 Quadrature rule for all subcylinders not containing the singularity $\mathbf{r}'$

We subdivide the cylinder into a total of three cylindrical regions and three washer-shaped regions, even if the singularity is at the center of the parent cylinder. Before subdividing, the distances from the three boundaries of the parent cylinder to the exclusion $V_\delta(\mathbf{r}')$ are measured. Let d be half of the minimum of the three distances. First, the radial direction ρ^{cyl}, measured from the singularity, is divided into two intervals with boundaries 0, $d+\delta$, and $\rho^{cyl}_{\max}$, where

$$\rho^{cyl}_{\max}(\varphi)=-\rho'(\varphi)+\sqrt{1-\mathbf{r}'^2_x-\mathbf{r}'^2_y+\rho'^2(\varphi)}\tag{4.8}$$

and

$$\rho'(\varphi)=\mathbf{r}'_x\cos(\varphi)+\mathbf{r}'_y\sin(\varphi).\tag{4.9}$$

This results in a cylindrical core containing the singularity with a washer, whose hole may be off center, wrapped around it. Second, the height of the parent cylinder is divided into the three intervals with boundaries at -1, $\mathbf{r}'_z-d-\delta$, $\mathbf{r}'_z+d+\delta$, and 1. The resulting six regions, with quadrature points, can be seen on the right of Fig. 4. Let S_1 and S_2 be the nonsingular subcylinders, given in cylinderical coordinates (ρ,φ,z) as $S_1=[0,d+\delta]\times[0,2\pi]\times[\mathbf{r}'_z+d+\delta,1]$, $S_2=[0,d+\delta]\times[0,2\pi]\times[-1,\mathbf{r}'_z-d-\delta]$, and let W_1,W_2,W_3 be the washers, given in cylindrical coordinates as $W_1=[d+\delta,\rho^{cyl}_{\max}]\times[0,2\pi]\times[\mathbf{r}'_z+d+\delta,1]$, $W_2=$

$[d+\delta,\rho^{cyl}_{\max}]\times[0,2\pi]\times[\mathbf{r}'_z-d-\delta,\mathbf{r}'_z+d+\delta]$, $W_3=[d+\delta,\rho^{cyl}_{\max}]\times[0,2\pi]\times[-1,\mathbf{r}'_z-d-\delta]$. Then (2.7) becomes

$$\begin{aligned}
&\int_{\Omega\setminus V_\delta(\mathbf{r}')}\frac{\phi_j(\mathbf{r})}{|\mathbf{r}-\mathbf{r}'|^k}d\mathbf{r}\\
&=\left(\int_\delta^{\frac{d+\delta}{\cos\theta}}\int_0^{\frac{\pi}{4}}+\int_\delta^{\frac{d+\delta}{\sin\theta}}\int_{\frac{\pi}{4}}^{\frac{3\pi}{4}}+\int_\delta^{-\frac{d+\delta}{\sin\theta}}\int_{\frac{3\pi}{4}}^{\pi}\right)\int_0^{2\pi}\frac{\phi_j(\mathbf{r})\rho^2\sin\theta}{|\mathbf{r}-\mathbf{r}'|^k}d\varphi d\theta d\rho\\
&\quad+\sum_{i=1}^{2}\int_{S_i}\frac{\phi_j(\mathbf{r})}{|\mathbf{r}-\mathbf{r}'|^k}\rho d\varphi dz d\rho+\sum_{i=1}^{3}\int_{W_i}\frac{\phi_j(\mathbf{r})}{|\mathbf{r}-\mathbf{r}'|^k}\rho d\varphi dz d\rho.
\end{aligned}\tag{4.10}$$

Only the middle subcylinder contains a singularity; the quadrature rule for it is described in the previous subsection and is mapped to this region. The remaining regions can be integrated in cylindrical coordinates (ρ^{cyl},φ,z), with Gaussian quadrature used in ρ^{cyl} and z, and the midpoint rule in φ. Specifically, with Gauss point-weights (t_ℓ,w^t_ℓ) defined on $[0,1]$, each cylinder with no singularity uses n^3_{cyl} points and weights in cylindrical coordinates given by

$$\begin{aligned}
&\left\{(t_i,\frac{2\pi(j+0.5)}{n_{cyl}},t_k):1\le i,j,k\le n_{cyl}\right\},\\
&\left\{\frac{2\pi}{n_{cyl}}w^t_iw^t_k:1\le i,j,k\le n_{cyl}\right\}.
\end{aligned}\tag{4.11}$$

Using n^ρ_w, n^φ_w, and n^z_w to denote the number of points on the washer regions in each direction, the quadrature points and weights are given in cylindrical coordinates by

$$\begin{aligned}
&\left\{(t_i,\frac{2\pi(j+0.5)}{n^\varphi_w},t_k):1\le i\le n^\rho_w,1\le j\le n^\varphi_w,1\le k\le n^z_w\right\},\\
&\left\{\frac{2\pi}{n^\varphi_w}w^t_iw^t_k:1\le i\le n^\rho_w,1\le j\le n^\varphi_w,1\le k\le n^z_w\right\}.
\end{aligned}\tag{4.12}$$

Since it is best to use twice as many points in the φ direction, let $n_w=n^\rho_w$ so that a total of $2n^3_w$ points and weights are on each washer. Counting all six subregions, the cylinder uses a total of $N=3n^3+2n^3_{cyl}+6n^3_w$ points; the points and weights are converted to Cartesian coordinates. Our code provides the option to allow further subdivisions in case a cylinder or washer has a dimension that is significantly larger than one of its other dimensions.

4.3 M-point tensor-product quadratures for a cylinder

To construct the quadrature weights defined in (2.6) for a set of tensor-product nodes corresponding to 1-D Gauss points on $[-1,1]$ or uniform points over $[0,2\pi]$, we will first define the interpolation functions. We will use Lagrange interpolation in ρ and z and

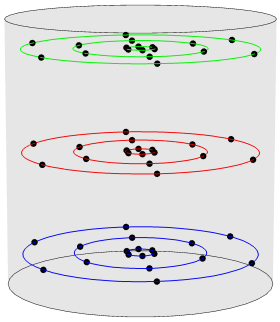

Figure 5: Interpolation points on the cylinder with circles when φ is a free variable and $m=3$ and $M=54$.

Fourier interpolation for φ. Let m_ρ, m_φ, and m_z be the number of sample points in ρ^{cyl}, φ, and z, respectively. Since twice as many points are needed in the φ direction, let $m=m_\rho$ so that $M=2m^3$ sample points are used. Shown in Fig. 5, the interpolation points are

$$\left\{(t_i,\frac{2\pi(j+0.5)}{m_\varphi},t_k):1\le i\le m_\rho,1\le j\le m_\varphi,1\le k\le m_z\right\}, \tag{4.13}$$

where t_ℓ are the Gauss points defined on $[0,1]$. For the basis functions, let $\ell_i^\rho(\rho)$ be the i^{th} Lagrange polynomial for ρ, given by

$$\ell_i^\rho(\rho)=\prod_{1\le p\le m_\rho,p\neq i}\frac{\rho-t_p}{t_i-t_p}. \tag{4.14}$$

The k^{th} Lagrange polynomial for z is similar. The Fourier interpolation polynomial for the φ direction can be shown to have the form

$$\ell_j^\varphi(\varphi)=\begin{cases}\frac{1}{m_\varphi}\frac{\sin(m_\varphi(\varphi-\varphi_j)/2)}{\sin((\varphi-\varphi_j)/2)}, & m_\varphi \text{ is odd and } \varphi\neq\varphi_j,\\ \frac{1}{m_\varphi}\frac{\sin(m_\varphi(\varphi-\varphi_j)/2)}{\sin((\varphi-\varphi_j)/2)}\cos((\varphi-\varphi_j)/2), & m_\varphi \text{ is even and } \varphi\neq\varphi_j,\\ 1, & \varphi=\varphi_j.\end{cases} \tag{4.15}$$

Multiplying the basis functions together yields

$$L_{i,j,k}^{cyl}(\rho,\varphi,z)=\ell_i^\rho(\rho)\ell_j^\varphi(\varphi)\ell_k^z(z). \tag{4.16}$$

Letting $\mathbf{r}$ be the Cartesian coordinates for (ρ,φ,z), $L_{i,j,k}(\mathbf{r})=L_{i,j,k}^{cyl}(\rho,\varphi,z)$. Then, renaming and reindexing $L_{i,j,k}(\mathbf{r})$ as $\phi_j(\mathbf{r})$, we get a set of basis functions that satisfies (2.3). Next, we use our N-point quadrature rule over the cylinder to integrate the basis functions against the singular kernal, as in (2.6). This produces the weights $w_{j,k}$. Finally, the integral over the cylinder with radius 1 and bases satisfying $z=-1$ and $z=1$ is given by (2.5).

5 M-point tensor-product quadratures for a sphere or ellipsoid

5.1 Quadrature rule over a sphere for singular kernal

We consider the unit sphere for Ω. In terms of (2.7), we want to calculate

$$\int_{\Omega\setminus V_\delta(\mathbf{r}')}\frac{\phi_j(\mathbf{r})}{|\mathbf{r}-\mathbf{r}'|^k}d\mathbf{r}=\int_\delta^{\rho_{\max}}\int_0^\pi\int_0^{2\pi}\frac{\phi_j(\mathbf{r})}{|\mathbf{r}-\mathbf{r}'|^k}\rho^2\sin(\theta)d\varphi d\theta d\rho, \tag{5.1}$$

where $\mathbf{r}'$ does not have to be at the sphere's center and $\rho_{\max}$ will be given later. Using spherical coordinates (ρ,φ,θ) to reduce the singularity, we use a midpoint rule for the azimuthal angle φ and Gauss quadrature for ρ and θ.

The n_φ points and weights for the azimuthal angle are given by

$$\varphi_k=2\pi\left(k+\frac{1}{2}\right)/n_\varphi,\quad w_k^\varphi=2\pi k/n_\varphi. \tag{5.2}$$

Let n_θ one-dimensional Gauss points and weights over $[0,1]$ be denoted by (t_j,w_j^t). Then, the points and weights (θ_j,w_j^θ) for the angle of inclination are given by

$$\theta_{j,k}=\pi t_j,\quad w_{j,k}^\theta=\pi w_j^t. \tag{5.3}$$

For a fixed singularity $\mathbf{r}'$, let

$$\rho'(\varphi,\theta)=\mathbf{r}'_x\cos(\varphi)\sin(\theta)+\mathbf{r}'_y\sin(\varphi)\sin(\theta)+\mathbf{r}'_z\cos(\theta). \tag{5.4}$$

Then, in terms of φ and θ, the maximum value of ρ is given by

$$\rho_{\max}(\varphi,\theta)=-\rho'(\varphi,\theta)+\sqrt{1-\mathbf{r}'^2_x-\mathbf{r}'^2_y-\mathbf{r}'^2_z+\rho'^2(\varphi,\theta)}. \tag{5.5}$$

Let n_ρ one-dimensional Gauss points and weights over $[0,1]$ be denoted by (t_i,w_i^t). Thus, for fixed angles φ_k and θ_j, we map a Gauss point-weight pair (t_i,w_i^t) to its corresponding radius and weight (ρ_i,w_i^r) by

$$\begin{aligned}\rho_{i,j,k}&=(\rho_{\max}(\varphi,\theta)-\rho_{\min})\,t_i+\rho_{\min},\\ w_{i,j,k}^\rho&=(\rho_{\max}(\varphi,\theta)-\rho_{\min})\,w_i^t.\end{aligned} \tag{5.6}$$

where $\rho_{\min}=\delta$ if a sphere around the singularity is excluded. Otherwise, $\rho_{\min}=0$. Matching indices, we now have a set of $N=n_\rho n_\varphi n_\theta$ points and weights on the sphere given by

$$\begin{aligned}&\{(\rho_{i,j,k},\theta_{j,k},\varphi_k):1\le i\le n_\rho,1\le j\le n_\varphi,1\le k\le n_\theta\},\\ &\{w_{i,j,k}^\rho w_{j,k}^\theta w_k^\varphi:1\le i\le n_\rho,1\le j\le n_\varphi,1\le k\le n_\theta\}.\end{aligned} \tag{5.7}$$

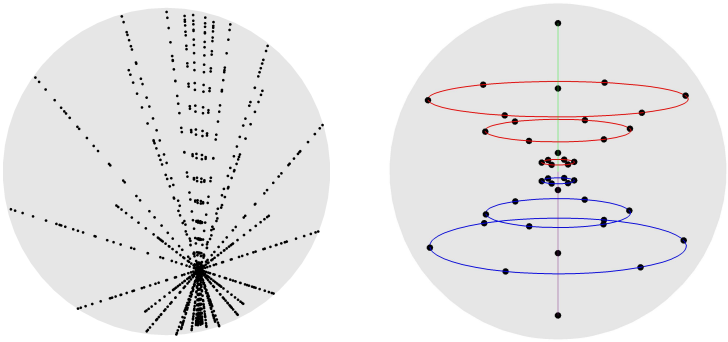

Figure 6: Sample points on the unit sphere. Left: Quadrature points when $\mathbf{r}'=(0.2,-0.3,-0.6)$ and $n=8$; right: Interpolation points with circles when φ is a free variable, $m=3$, and $M=42$.

Letting $n=n_\varphi=n_\theta$, we take $n_\rho=2n$ for a total of $N=2n^3$ points to get the best results. The points are converted to Cartesian coordinates. A set of quadrature points on the unit sphere is depicted in Fig. 6.

A similar method can be used to find a set of quadrature points on an ellipse by scaling the axis of the ellipse to a sphere. Letting $n=n_\rho$, we take $n_\varphi=n_\theta=2n$ for a total of $N=4n^3$ points to get the best results. The distribution of quadrature points is similar to the distribution for the sphere, shown in Fig. 6.

5.2 M-point tensor-product quadratures for a sphere

Similarly, to construct the quadrature weights defined in (2.6) for a tensor product nodes of 1-D Gauss points on $[-1,1]$ or uniform points over $[0,\pi]$ or $[0,2\pi]$, we will first define the interpolation functions. We will use Lagrange polynomials in ρ and the double Fourier basis described in [3] and [4] for φ and θ. Let m_ρ, m_φ, and m_θ be the number of sample points in ρ, φ, and θ, respectively. If m is specified for the sphere then $m=m_\rho=m_\varphi=m_\theta$. Tests have shown that $m_\varphi=m_\theta$ gives the best results. Shown in Fig. 6, a brief, initial description of the interpolation points is given by

$$\left\{\left(t_i,\frac{\pi j}{m_\varphi},\frac{\pi k}{m_\theta}\right):1\le i\le m_\rho,0\le j\le 2m_\varphi-1,0\le k\le m_\theta\right\}. \tag{5.8}$$

where t_ℓ are the m_ρ Gauss points defined on $[0,1]$. For the basis functions, let $\ell_i^\rho(\rho)$ be the i^{th} Lagrange polynomial for ρ, given by

$$\ell_i^\rho(\rho)=\prod_{1\le p\le m_\rho,p\ne i}\frac{\rho-t_p}{t_i-t_p}. \tag{5.9}$$

Defining

$$\ell_{p,q,k}^\theta(\theta)=\begin{cases}\sin(q\theta_k)\sin(q\theta), & p \text{ is odd},\\ \frac{1}{c_q c_k}\cos(q\theta_k)\cos(q\theta), & p \text{ is even},\end{cases} \tag{5.10}$$

where $c_q=2$ if $q=0$ or m_θ and $c_q=1$ otherwise, the basis function for φ and θ is given by

$$\ell_{j,k}^{\varphi,\theta}(\varphi,\theta)=\frac{1}{m_\varphi m_\theta}\sum_{p=0}^{2m_\varphi-1}\sum_{q=\mathrm{mod}(p,2)}^{m_\theta-\mathrm{mod}(p,2)}\ell_{p,q,k}^{\theta}(\theta)e^{im_\varphi(\varphi-\varphi_j)}, \tag{5.11}$$

where $i=\sqrt{-1}$ in this equation and only this equation. Multiplying the basis functions together yields

$$L_{i,j,k}^{sph}(\rho,\varphi,\theta)=\ell_i^\rho(\rho)\ell_{j,k}^{\varphi,\theta}(\varphi,\theta). \tag{5.12}$$

Letting $\mathbf{r}$ be the Cartesian coordinates for (ρ,φ,θ), $L_{i,j,k}(\mathbf{r})=L_{i,j,k}(\rho,\varphi,\theta)$. Renaming and reindexing $L_{i,j,k}(\mathbf{r})$ as $\phi_j(\mathbf{r})$, we get a set of basis functions that satisfies (2.3). Then, the interpolation formula for $f(\mathbf{r})$ is

$$f(\mathbf{r})\approx\sum_{i=1}^{m_\rho}\sum_{j=0}^{2m_\varphi-1}\sum_{k=0}^{m_\theta}f(\rho_i,\varphi_j,\theta_k)L_{i,j,k}(\rho,\varphi,\theta). \tag{5.13}$$

This formula is valid unless the Kronecker delta property is needed; there are many terms in the summation that share the same sample point if we consider Cartesian coordinates. Specifically, taking $k=0$ or m_θ and fixing i in $(\rho_i,\varphi_j,\theta_k)$ determines the sample point regardless of the value j takes. Thus, the basis functions fail to satisfy the Kronecker delta property in Cartesian coordinates. After calculating the weights according to (2.6) for the $2m_\rho m_\varphi(m_\theta+1)$ points given in (5.8), we determine which ones are not unique and add them together; the integral is then calculated with $M=m_\rho(2m_\varphi(m_\theta-1)+2)$ distinct points in Cartesian coordinates according to (2.5). This is equivalent to consolidating all basis functions with $k=0$ or m_θ and defining a new one for each i by

$$\hat{L}_{i,k}(\rho,\theta)=\sum_{j=0}^{2m_\varphi-1}L_{i,j,k}(\rho,\varphi,\theta). \tag{5.14}$$

With an implied change of coordinates, the basis functions in the new interpolation formula

$$\begin{aligned}f(\mathbf{r})\approx\sum_{i=1}^{m_\rho}\Bigg(&f(\rho_i,\varphi_0,\theta_0)\hat{L}_{i,0}(\rho,\theta)+f(\rho_i,\varphi_0,\theta_{m_\theta})\hat{L}_{i,m_\theta}(\rho,\theta)\\&+\sum_{k=1}^{m_\theta-1}\sum_{j=0}^{2m_\varphi-1}f(\rho_i,\varphi_j,\theta_k)L_{i,j,k}(\rho,\varphi,\theta)\Bigg)\end{aligned} \tag{5.15}$$

satisfy the Kronecker delta property in Cartesian coordinates. In practice, we have obtained the same results regardless of whether we consolidate the points or use them with a pseudo-Kronecker delta property.

For interpolation over an ellipsoid, the interpolation points and basis functions defined on the sphere are used with mappings between the sphere and ellipsoid.

6 Algorithm outline

The algorithm for calculating the weights in (2.6) does not heavily depend on the shape of the domain Ω. Here, we will provide an outline of the algorithm with some notes about what considerations each domain requires. While similar, considerations for the rectangular prism and ellipsoid are not given here.

The input to the algorithm consists in the dimensions of Ω, the location of the singularity $\mathbf{r}'$, the radius δ of the spherical exclusion V_δ, the number m of interpolation points in each direction, the number n of one dimensional brute-force quadrature points in spherical coordinates for the subregion containing the singularity, and the number n_{reg}, n_{cyl}, or n_w of one dimensional brute-force quadrature points for any subregions not containing the singularity. The dimensions and directions are defined in Cartesian, cylindrical, and spherical coordinates for the cuboid, cylindrical, and spherical regions, respectively. Spherical domains do not have any subregions.

If the domain is not spherical, the first step is to determine if subdivisions are necessary given the location of the singularity $\mathbf{r}'$. If they are, the dimensions of each subregion must be calculated. If desired, these subregions can be further subdivided until no region has a single dimension that is significantly larger than any other dimension.

After all required subregions are specified, the brute-force quadrature rule is made. Points and weights are calculated for subregions not containing the singularity according to formula (3.7) for the cube and formulas (4.11) and (4.12) for the cylinder. For all domains, there is a subregion, perhaps identical to Ω, that contains the singularity. Using spherical coordinates, points and weights are calculated for this subregion according to the formulas (3.6), (4.7), and (5.7) for the cuboid, cylindrical, and spherical regions, respectively. Note that the formula for the cuboid gives the points and weights for only one of the six pyramids that make up the cuboid.

Next, the sample points for interpolation are calculated according to (3.10), (4.13), and (5.8) for the cuboid, cylindrical, and spherical regions, respectively. The basis functions are defined by these interpolation points so there is no need to construct them.

Finally, the desired tensor-product quadrature rule is made by calculating the brute force integrals of the basis functions against the singular kernel, according to (2.6). The points for the tensor-product quadrature rule are the interpolation points and the weights are the $w_{j,k}$ in (2.6). For the sphere, the number of sample points and weights can be reduced by combining the weights that correspond to the same points in Cartesian coordinates.

The output from the algorithm is the set of sample points $\mathbf{r}_j$ and corresponding weights $w_{j,k}$. When implemented in computer code, these points and weights can be saved to a file for use in the future. Thus, the algorithm needs to only be used once for each set of inputs even if there are many integrals to calculate. If the domain of integration has different dimensions from the one used to calculate the weights $w_{j,k}$, the Jacobian given by (2.8) can be used to calculate the correct integral at runtime.

7 Numerical results

We use our method to approximate several integrals, subdividing the domain when necessary as in Fig. 2 and Fig. 4. For convenience, let $R=|\mathbf{r}-\mathbf{r}'|$ in this section. In each test we increase the value of M and place the singularity at the interpolation point closest to the boundary to show the most difficult case; as M increases, the singularity will get closer to the boundary. When the denominator contains R^3, even if we reduce the order of the singularity in some way, δ is taken as half of the distance from the singularity to the boundary; otherwise $\delta=0$. All reference solutions are calculated with our method by performing the brute-force integral with twice as many quadrature points in each direction. While not reported here, we also check our results against Mathematica's NIntegrate function to make sure our method converges to the same value Mathematica's does [5].

There are three tests we perform for when the domain is a cube, cylinder, or sphere; we have obtained good results for when the domain is a rectangular prism or an ellipsoid, but they are not provided here. First, we take $f(\mathbf{r})=\cos(R)$ in (2.1) and consider the kernels $1/R$, $1/R^2$, and $1/R^3$. Second, we repeat the test for $\sin(R)$. Since $\sin(R)$ has a cusp at $R=0$, we take $f(\mathbf{r})=\sin(R)/R$ and consider the kernels 1, $1/R$, $1/R^2$. While not necessary to get good convergence for $\sin(R)/R^3$, we will take δ to be nonzero to illustrate good convergence for when an exponential function is split into sine and cosine by Euler's formula.

Third, we show a convergence result from a more realistic scenario. Consider a Green's function defined by the matrix

$$\mathbf{G}(\mathbf{r},\mathbf{r}')=\left(\mathbf{I}+\frac{1}{k^2}\nabla\nabla\right)\frac{e^{-ikR}}{4\pi R}, \tag{7.1}$$

where $\mathbf{I}$ is the identity matrix. This is the Green's function in [1]. Let $\mathbf{u}$ be the unit vector in the direction of $\mathbf{r}-\mathbf{r}'$. Then the hypersingular part of $\mathbf{G}(\mathbf{r},\mathbf{r}')$ has the same behavior as

$$\mathbf{H}(\mathbf{r},\mathbf{r}')=(\mathbf{I}-3\mathbf{u}\otimes\mathbf{u})\frac{\cos(R)}{R^3}. \tag{7.2}$$

$\mathbf{H}(\mathbf{r},\mathbf{r}')$ is a symmetric matrix whose entries are defined by

$$\mathbf{H}_{u,v}(\mathbf{r},\mathbf{r}')=\left(\delta_{uv}-3\frac{(\mathbf{r}_u-\mathbf{r}'_u)(\mathbf{r}_v-\mathbf{r}'_v)}{R^2}\right)\frac{\cos(R)}{R^3}, \tag{7.3}$$

where $\delta_{u,v}$ is the Kronecker delta and u,v take the values x,y,z. As the second term in the parenthesis depends on the variable of integration, we build on (2.6) by defining

$$w_j^{u,v}=\sum_{i=1}^{N}\left(\delta_{uv}-3\frac{(\mathbf{r}_u-\mathbf{r}'_u)(\mathbf{r}_v-\mathbf{r}'_v)}{|\mathbf{r}_i-\mathbf{r}'|^2}\right)\frac{\phi_j(\hat{\mathbf{r}}_i)}{|\hat{\mathbf{r}}_i-\mathbf{r}'|^3}\hat{w}_i. \tag{7.4}$$

The difference in the weights $w_j^{u,v}$ removes the singularity from the diagonal entries of $\mathbf{H}(\mathbf{r},\mathbf{r}')$ so the integral over any sphere centered at $\mathbf{r}'$ is zero. Since, in a realistic scenario, $\mathbf{H}(\mathbf{r},\mathbf{r}')$ is multiplied by a basis function that destroys any symmetry, we take $\hat{\mathbf{H}}(\mathbf{r},\mathbf{r}') = b(\mathbf{r})\mathbf{H}(\mathbf{r},\mathbf{r}')$, where $b(\mathbf{r}) = (\mathbf{r}_x+1/2)^2(\mathbf{r}_y+1/4)^2(\mathbf{r}_z+1/8)^2+1$. Thus, we use an exclusion $V_\delta(\mathbf{r}')$ to get good convergence. Then, we can integrate the entries of $\hat{\mathbf{H}}(\mathbf{r},\mathbf{r}')$ by the interpolation formula

$$\int_{\Omega\setminus V_\delta(\mathbf{r}')} \hat{\mathbf{H}}_{u,v}(\mathbf{r},\mathbf{r}')d\mathbf{r} \approx \sum_{j=1}^{M} b(\mathbf{r}_j)\cos(|\mathbf{r}_j-\mathbf{r}'|)w_j^{u,v}. \tag{7.5}$$

7.1 Numerical results for when Ω is a cube

We take $\Omega = [-1/4,1/4]^3$ when integrating $\hat{\mathbf{H}}_{u,v}(\mathbf{r},\mathbf{r}')$, but take $\Omega = [-1,1]^3$ for $f(\mathbf{r}) = \cos(R)$ or $f(\mathbf{r}) = \sin(R)/R$, for which machine error was quickly reached. Convergence results are given in Fig. 7 for the first two tests and in Fig. 8 for the third test. Our approximations are calculated using $n = n_{reg} = 32$ for all tests except $\cos(R)/R^3$ and $\hat{\mathbf{H}}_{u,v}(\mathbf{r},\mathbf{r}')$; in

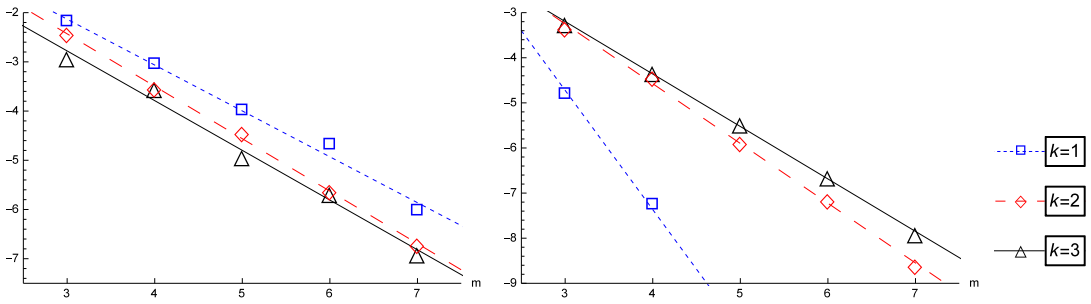

Figure 7: The $\log_{10}$ relative error of the integrals of $\cos(R)/R^k$ (left) and $\sin(R)/R^k$ (right) when Ω is the cube $\Omega = [-1,1]^3$. $M = m^3$ sample points are used in (2.5).

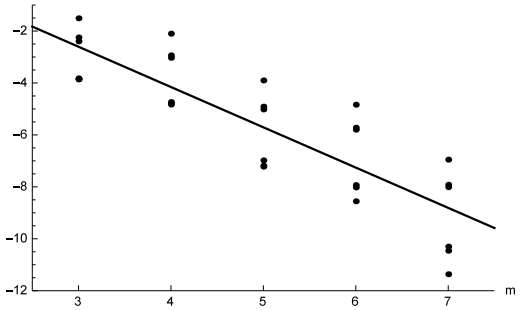

Figure 8: The $\log_{10}$ relative error of the integral of the entries of $\hat{\mathbf{H}}(\mathbf{r},\mathbf{r}')$ when Ω is the cube $\Omega = [-1/4,1/4]^3$. Each point corresponds to an entry of $\hat{\mathbf{H}}$ for a given m; the line is a linear fit for all points. $M = m^3$ sample points are used in (2.5).

these cases, $n=64$. N is 53,248 and 1,601,536, respectively. The code is given permission to subdivide the nonsingular regions further, which will increase N.

7.2 Numerical results for when Ω is a cylinder

Ω is a cylinder of radius 1/4 and height 1/2. Convergence results are given in Fig. 9 for the first two tests and in Fig. 10 for the third test. Our approximations are calculated using $n=n_{cyl}=16$ and $n_w=64$ for all tests except $\cos(R)/R^3$ and $\hat{\mathbf{H}}_{u,v}(\mathbf{r},\mathbf{r}')$; in these cases, $n=64$. N is 3,166,208 and 3,940,352, respectively. The code is given permission to subdivide the nonsingular regions further, which will increase N.

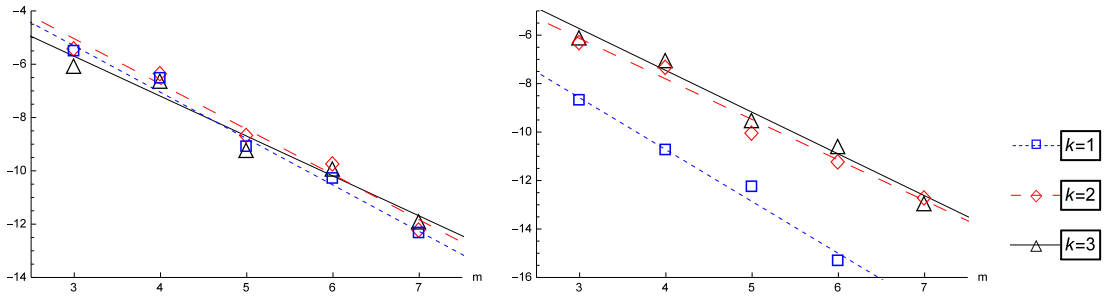

Figure 9: The $\log_{10}$ relative error of the integrals of $\cos(R)/R^k$ (left) and $\sin(R)/R^k$ (right) when Ω is a cylinder. $M=2m^3$ sample points are used in (2.5).

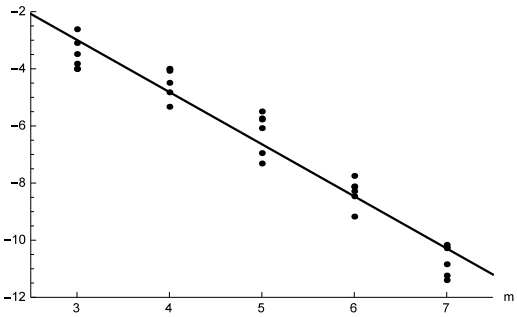

Figure 10: The $\log_{10}$ relative error of the integral of the entries of $\hat{\mathbf{H}}(\mathbf{r},\mathbf{r}')$ when Ω is a cylinder. Each point corresponds to an entry of $\hat{\mathbf{H}}$ for a given m; the line is a linear fit for all points. $M=2m^3$ sample points are used in (2.5).

7.3 Numerical results for when Ω is a sphere

Ω is a sphere of radius 1 when $f(\mathbf{r})=\cos(R)$ or $f(\mathbf{r})=\sin(R)/R$, but Ω is a sphere of radius 1/4 when integrating $\hat{\mathbf{H}}_{u,v}(\mathbf{r},\mathbf{r}')$. Convergence results are given in Fig. 11 for the first two tests and in Fig. 12 for the third test. Our approximations are calculated using

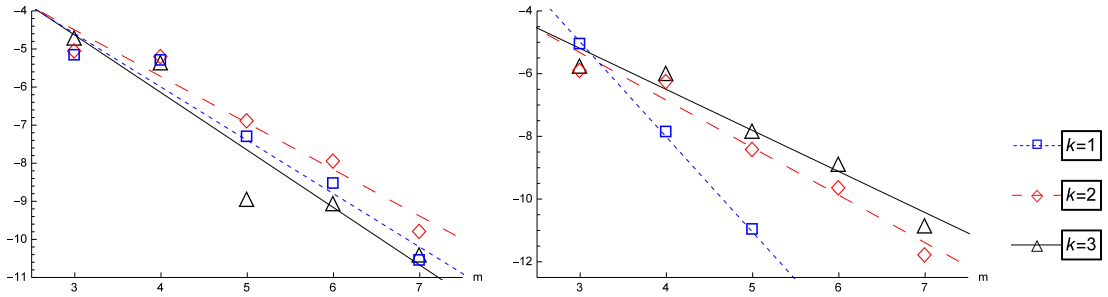

Figure 11: The $\log_{10}$ relative error of the integrals of $\cos(R)/R^k$ (left) and $\sin(R)/R^k$ (right) when Ω is a sphere. $M=m_\rho(2m_\varphi(m_\theta-1)+2)$ sample points are used in (2.5).

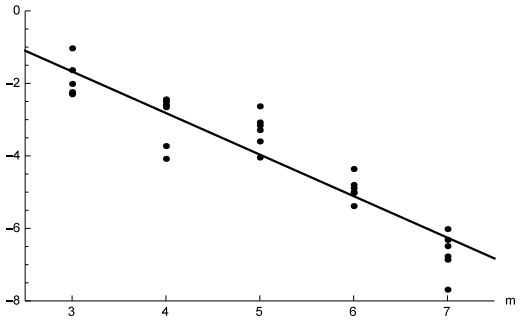

Figure 12: The $\log_{10}$ relative error of the integral of the entries of $\hat{\mathbf{H}}(\mathbf{r},\mathbf{r}')$ when Ω is a sphere. Each point corresponds to an entry of $\hat{\mathbf{H}}$ for a given m; the line is a linear fit for all points. $M=m_\rho(2m_\varphi(m_\theta-1)+2)$ sample points are used in (2.5).

$n=64$ for all tests. $N=524{,}288$. It is not possible to give the code permission to subdivide the sphere.

8 Conclusion

In this paper we have proposed algorithms to generate accurate and efficient tensor-product quadrature formula for hypersingular functions over cubes, rectangles, spheres, and cylinders with a spherical exclusion volume. The quadrature rule is derived from direct brute-force quadratures through an interpolation technique for the smooth part of the integrand. The resulting tensor-product quadrature, which can be pre-computed and tabulated, and can reproduce the brute-force quadrature results with only a small number of samples of the integrand.

Relevant work includes applying the tensor-product quadrature to construct Nyström collocation methods for hypersingular volume integral equations (VIEs) as in the electromagnetic scattering of a random array of multiple simple objects in the design of metamaterials [1], where the contribution of the integral over the exclusion volume V_δ is also addressed for the VIEs of the Maxwell equations.

Finally, the codes which produce the quadrature weights for the three domains are available from the authors.

Acknowledgments

The authors acknowledge the support of the US Army Office of Research (Grant No. W911NF-14-1-0297). Authors thank Jie Shen for helpful discussion on interpolation over spheres.

Appendices

A Rotation matrices

The cube, cylinder, and sphere have rotational symmetry. We take advantage of this by providing the weights $w_{j,k}$ for when the singularity is located at certain interpolation points. When the singularity is located at an interpolation point for which there is no table, we provide a rotation map R that rotates the domain so that the singularity coincides with an interpolation point that has a table of weights. Let the rotation matrix R be defined by $R=R_x(\alpha)R_y(\beta)R_z(\gamma)$ so the space is first rotated around the z-axis; second, it is rotated around the y-axis; last, it is rotated around the x-axis. The multipliers $R_x(\alpha)$, $R_y(\beta)$, and $R_z(\gamma)$ are respectively given by:

$$\begin{bmatrix} 1 & 0 & 0 \\ 0 & \cos(\alpha) & -\sin(\alpha) \\ 0 & \sin(\alpha) & \cos(\alpha) \end{bmatrix}, \begin{bmatrix} \cos(\beta) & 0 & \sin(\beta) \\ 0 & 1 & 0 \\ -\sin(\beta) & 0 & \cos(\beta) \end{bmatrix}, \begin{bmatrix} \cos(\gamma) & -\sin(\gamma) & 0 \\ \sin(\gamma) & \cos(\gamma) & 0 \\ 0 & 0 & 1 \end{bmatrix}. \quad \text{(A.1)}$$

Note that 3×3 rotation matrices do not form a commutative group, i.e., $R_x(\alpha)R_y(\beta)R_z(\gamma)\neq R_z(\gamma)R_y(\beta)R_x(\alpha)$ in general. For each location of the singularity, corresponding rotation matrices are given in the appendices.

For example, the quadrature formula recorded in the tables for a singularity at node $\mathbf{r}_i'$ is

$$\int_{\Omega\setminus V_\delta(\mathbf{r}_i')} \frac{f(\mathbf{r})}{|\mathbf{r}-\mathbf{r}_i'|^k} d\mathbf{r} \approx \sum_{j=1}^{M} f(\mathbf{r}_j) w_{j,k}, \quad \text{(A.2)}$$

and a symmetric node $\mathbf{r}_i''$ is related by a rotation matrix $R=R_x(\alpha)R_y(\beta)R_z(\gamma)$ according to

$$\mathbf{r}_i''=R\mathbf{r}_i'. \quad \text{(A.3)}$$

Then, the integral with a singularity located at $\mathbf{r}_i''$ can be done with the same quadrature nodes and weights as in (A.2) with the help of the rotation matrix R:

$$\int_{\Omega\setminus V_\delta(\mathbf{r}_i'')} \frac{f(\mathbf{r})}{|\mathbf{r}-\mathbf{r}_i''|^k} d\mathbf{r} \approx \sum_{j=1}^{M} f(R\mathbf{r}_j) w_{j,k}. \quad \text{(A.4)}$$

B Integration quadrature nodes and weights for singular kernels over a cube

We provide the quadrature nodes (also the interpolation nodes) and weights for integrating over $[-1,1]^3$ according to Eq. (2.4) when $M=27$ and the singularity corresponds to a quadrature node. The four cases for the weights correspond to when the singularity is at the origin, the center of a face, the center of an edge, and a corner. When the singularity is at a quadrature node that we do not list, the corresponding weights can be obtained by rotating the cube in Fig. 3 around the x, y, and z axes by α, β, and γ, respectively.

The listed quadrature weights over the tensor product nodes are converted from the brute-force integration using $n=32$ except when $\delta>0$. For $\delta>0$, $n=64$ is chosen to handle integrating $1/R^3$ accurately. $n_{reg}=32$ and the code is allowed to subdivide the cube further in all cases. Refer to Section 3 for the meanings of brute-force quadrature parameters n and n_{reg}.

Table 1: Quadrature nodes (x,y,z) on the cube $[-1,1]^3$ with the required rotation angles (α,β,γ) to rotate a node to its representative symmetric node (identified with (0,0,0) angles), for which quadrature weight table is given.

Index	x	y	z	α	β	γ	Index	x	y	z	α	β	γ
1	$-\sqrt{3/5}$	$-\sqrt{3/5}$	$-\sqrt{3/5}$	0	$-\pi/2$	π	15	0	0	$\sqrt{3/5}$	0	$-\pi/2$	0
2	$-\sqrt{3/5}$	$-\sqrt{3/5}$	0	0	0	π	16	0	$\sqrt{3/5}$	$-\sqrt{3/5}$	0	$\pi/2$	0
3	$-\sqrt{3/5}$	$-\sqrt{3/5}$	$\sqrt{3/5}$	0	0	π	17	0	$\sqrt{3/5}$	0	0	0	$\pi/2$
4	$-\sqrt{3/5}$	0	$-\sqrt{3/5}$	$\pi/2$	0	π	18	0	$\sqrt{3/5}$	$\sqrt{3/5}$	0	$-\pi/2$	0
5	$-\sqrt{3/5}$	0	0	0	0	π	19	$\sqrt{3/5}$	$-\sqrt{3/5}$	$-\sqrt{3/5}$	π	0	0
6	$-\sqrt{3/5}$	0	$\sqrt{3/5}$	$-\pi/2$	0	π	20	$\sqrt{3/5}$	$-\sqrt{3/5}$	0	π	0	0
7	$-\sqrt{3/5}$	$\sqrt{3/5}$	$-\sqrt{3/5}$	0	π	0	21	$\sqrt{3/5}$	$-\sqrt{3/5}$	$\sqrt{3/5}$	0	0	$-\pi/2$
8	$-\sqrt{3/5}$	$\sqrt{3/5}$	0	0	π	0	22	$\sqrt{3/5}$	0	$-\sqrt{3/5}$	$-\pi/2$	0	0
9	$-\sqrt{3/5}$	$\sqrt{3/5}$	$\sqrt{3/5}$	0	$-\pi/2$	0	23	$\sqrt{3/5}$	0	0	0	0	0
10	0	$-\sqrt{3/5}$	$-\sqrt{3/5}$	0	$-\pi/2$	π	24	$\sqrt{3/5}$	0	$\sqrt{3/5}$	$\pi/2$	0	0
11	0	$-\sqrt{3/5}$	0	0	0	$-\pi/2$	25	$\sqrt{3/5}$	$\sqrt{3/5}$	$-\sqrt{3/5}$	$-\pi/2$	0	0
12	0	$-\sqrt{3/5}$	$\sqrt{3/5}$	0	$\pi/2$	π	26	$\sqrt{3/5}$	$\sqrt{3/5}$	0	0	0	0
13	0	0	$-\sqrt{3/5}$	0	$\pi/2$	0	27	$\sqrt{3/5}$	$\sqrt{3/5}$	$\sqrt{3/5}$	0	0	0
14	0	0	0	0	0	0							

Table 2: Weights for when the singularity is at $(0,0,0)$. This table can only be used when the singularity is at this location, which corresponds to index 14 and the red point in Fig. 3. $\delta_0=0$ and $\delta_1=(1-\sqrt{3/5})/2$.

Index	$1/R,\delta_0$	$1/R^2,\delta_0$	$1/R^2,\delta_1$	$1/R^3,\delta_1$	Index	$1/R,\delta_0$	$1/R^2,\delta_0$	$1/R^2,\delta_1$	$1/R^3,\delta_1$
1	0.13157093	0.10342060	0.10342059	0.08372364	15	0.57495100	0.80206626	0.80040909	1.25774485
2	0.25835351	0.25161840	0.25161628	0.25743060	16	0.25835351	0.25161840	0.25161628	0.25743060
3	0.13157093	0.10342060	0.10342059	0.08372364	17	0.57495100	0.80206626	0.80040909	1.25774485
4	0.25835351	0.25161840	0.25161628	0.25743060	18	0.25835351	0.25161840	0.25161628	0.25743060
5	0.57495100	0.80206626	0.80040909	1.25774485	19	0.13157093	0.10342060	0.10342059	0.08372364
6	0.25835351	0.25161840	0.25161628	0.25743060	20	0.25835351	0.25161840	0.25161628	0.25743060
7	0.13157093	0.10342060	0.10342059	0.08372364	21	0.13157093	0.10342060	0.10342059	0.08372364
8	0.25835351	0.25161840	0.25161628	0.25743060	22	0.25835351	0.25161840	0.25161628	0.25743060
9	0.13157093	0.10342060	0.10342059	0.08372364	23	0.57495100	0.80206626	0.80040909	1.25774485
10	0.25835351	0.25161840	0.25161628	0.25743060	24	0.25835351	0.25161840	0.25161628	0.25743060
11	0.57495100	0.80206626	0.80040909	1.25774485	25	0.13157093	0.10342060	0.10342059	0.08372364
12	0.25835351	0.25161840	0.25161628	0.25743060	26	0.25835351	0.25161840	0.25161628	0.25743060
13	0.57495100	0.80206626	0.80040909	1.25774485	27	0.13157093	0.10342060	0.10342059	0.08372364
14	1.91779381	6.68906539	5.28278287	18.54405540					

Table 3: Weights for when the singularity is at $(\sqrt{3/5},0,0)$. After a rotation, this table can be used when the singularity is at index 5, 11, 13, 15, 17, or 23: a black point in Fig. 3. $\delta_0=0$ and $\delta_1=(1-\sqrt{3/5})/2$.

Index	$1/R,\delta_0$	$1/R^2,\delta_0$	$1/R^2,\delta_1$	$1/R^3,\delta_1$	Index	$1/R,\delta_0$	$1/R^2,\delta_0$	$1/R^2,\delta_1$	$1/R^3,\delta_1$
1	0.08996882	0.04631985	0.04631985	0.02264362	15	0.41410360	0.40810772	0.40811194	0.42670704
2	0.15511179	0.08260310	0.08260099	0.03630368	16	0.21019086	0.16563488	0.16563489	0.13531770
3	0.08996882	0.04631985	0.04631985	0.02264362	17	0.41410360	0.40810772	0.40811194	0.42670704
4	0.15511179	0.08260310	0.08260099	0.03630368	18	0.21019086	0.16563488	0.16563489	0.13531770
5	0.26343083	0.12701538	0.12535821	0.02324414	19	0.16373121	0.16276074	0.16275862	0.17137800
6	0.15511179	0.08260310	0.08260099	0.03630368	20	0.37123205	0.54485770	0.54319419	0.91958196
7	0.08996882	0.04631985	0.04631985	0.02264362	21	0.16373121	0.16276074	0.16275862	0.17137800
8	0.15511179	0.08260310	0.08260099	0.03630368	22	0.37123205	0.54485770	0.54319419	0.91958196
9	0.08996882	0.04631985	0.04631985	0.02264362	23	1.35695256	5.55396694	4.14271291	16.24680983
10	0.21019086	0.16563488	0.16563489	0.13531770	24	0.37123205	0.54485770	0.54319419	0.91958196
11	0.41410360	0.40810772	0.40811194	0.42670704	25	0.16373121	0.16276074	0.16275862	0.17137800
12	0.21019086	0.16563488	0.16563489	0.13531770	26	0.37123205	0.54485770	0.54319419	0.91958196
13	0.41410360	0.40810772	0.40811194	0.42670704	27	0.16373121	0.16276074	0.16275862	0.17137800
14	0.93352594	1.32753647	1.33085081	2.03644181					

Table 4: Weights for when the singularity is at $(\sqrt{3/5},\sqrt{3/5},0)$. After a rotation, this table can be used when the singularity is at index 2, 4, 6, 8, 10, 12, 16, 18, 20, 22, 24, or 26: a green point in Fig. 3. $\delta_0=0$ and $\delta_1=(1-\sqrt{3/5})/2$.

Index	$1/R,\delta_0$	$1/R^2,\delta_0$	$1/R^2,\delta_1$	$1/R^3,\delta_1$	Index	$1/R,\delta_0$	$1/R^2,\delta_0$	$1/R^2,\delta_1$	$1/R^3,\delta_1$
1	0.07379387	0.03177118	0.03177118	0.01378748	15	0.33585737	0.26551138	0.26551138	0.21926419
2	0.12507486	0.05746573	0.05746362	0.02784906	16	0.26261177	0.26455768	0.26456192	0.28495605
3	0.07379387	0.03177118	0.03177118	0.01378748	17	0.60390858	0.89940509	0.90273210	1.45051090
4	0.14366304	0.07368413	0.07368413	0.03565473	18	0.26261177	0.26455768	0.26456192	0.28495605
5	0.24730547	0.13008899	0.13009321	0.05325413	19	0.09707427	0.05146506	0.05146294	0.02184551
6	0.14366304	0.07368413	0.07368413	0.03565473	20	0.16408356	0.07711557	0.07545206	0.01645008
7	0.09707427	0.05146506	0.05146294	0.02184551	21	0.09707427	0.05146506	0.05146294	0.02184551
8	0.16408356	0.07711557	0.07545206	0.01645008	22	0.26261177	0.26455768	0.26456192	0.28495605
9	0.09707427	0.05146506	0.05146294	0.02184551	23	0.60390858	0.89940509	0.90273210	1.45051090
10	0.14366304	0.07368413	0.07368413	0.03565473	24	0.26261177	0.26455768	0.26456192	0.28495605
11	0.24730547	0.13008899	0.13009321	0.05325413	25	0.24064330	0.37443703	0.37276717	0.68642402
12	0.14366304	0.07368413	0.07368413	0.03565473	26	0.98274360	4.74857993	3.33233538	14.52260598
13	0.33585737	0.26551138	0.26551138	0.21926419	27	0.24064330	0.37443703	0.37276717	0.68642402
14	0.66435641	0.66448876	0.66448032	0.71570571					

Table 5: Weights for when the singularity is at $(\sqrt{3/5},\sqrt{3/5},\sqrt{3/5})$. After a rotation, this table can be used when the singularity is at index 1, 3, 7, 9, 19, 21, 25, or 27: a yellow point in Fig. 3. $\delta_0=0$ and $\delta_1=(1-\sqrt{3/5})/2$.

Index	$1/R,\delta_0$	$1/R^2,\delta_0$	$1/R^2,\delta_1$	$1/R^3,\delta_1$	Index	$1/R,\delta_0$	$1/R^2,\delta_0$	$1/R^2,\delta_1$	$1/R^3,\delta_1$
1	0.06388138	0.02375271	0.02375271	0.00878139	15	0.42166601	0.43204064	0.43203217	0.48097382
2	0.11795846	0.05074363	0.05074364	0.02204209	16	0.15472747	0.08083987	0.08084411	0.03115808
3	0.07830974	0.03614458	0.03614246	0.01783615	17	0.42166601	0.43204064	0.43203217	0.48097382
4	0.11795846	0.05074363	0.05074364	0.02204209	18	0.39217690	0.61424481	0.61758453	1.04337202
5	0.22939304	0.11717253	0.11717252	0.05603658	19	0.07830974	0.03614458	0.03614246	0.01783615
6	0.15472747	0.08083987	0.08084411	0.03115808	20	0.15472747	0.08083987	0.08084411	0.03115808
7	0.07830974	0.03614458	0.03614246	0.01783615	21	0.10210600	0.04694253	0.04527267	0.01542046
8	0.15472747	0.08083987	0.08084411	0.03115808	22	0.15472747	0.08083987	0.08084411	0.03115808
9	0.10210600	0.04694253	0.04527267	0.01542046	23	0.42166601	0.43204064	0.43203217	0.48097382
10	0.11795846	0.05074363	0.05074364	0.02204209	24	0.39217690	0.61424481	0.61758453	1.04337202
11	0.22939304	0.11717253	0.11717252	0.05603658	25	0.10210600	0.04694253	0.04527267	0.01542046
12	0.15472747	0.08083987	0.08084411	0.03115808	26	0.39217690	0.61424481	0.61758453	1.04337202
13	0.22939304	0.11717253	0.11717252	0.05603658	27	0.73106704	4.17027622	2.74902210	13.21194489
14	0.53678126	0.42605412	0.42605414	0.35629233					

Finally, the size δ of the exclusion volume V_δ is specified in the tables as either $\delta_0 = 0$ or $\delta_1 = (1-\sqrt{3/5})/2$, which is the half of the smallest distance from the quadrature nodes to the boundary of the cube.

C Integration quadrature nodes and weights for singular kernels over a cylinder

We provide the quadrature nodes (also the interpolation nodes) and weights for integrating over a cylinder with radius 1 that goes from $z=-1$ to $z=1$ according to Eq. (2.4) when $M=54$ and the singularity corresponds to an quadrature node. The six cases for the weights correspond to when $z=0$ or at its maximum and all values for ρ^{cyl}. When the singularity is at a quadrature node that we do not list, the corresponding weights can be obtained by rotating the cylinder in Fig. 5 around the x, y, and z axes by α, β, and γ, respectively.

The listed quadrature weights over the tensor product nodes are converted from the brute-force integration using $n = n_{cyl} = 16$ and $n_w = 64$ except when $\delta > 0$. Then $n = 64$ to handle integrating $1/R^3$ accurately. Refer to Section 4 for the meanings of brute-

Table 6: Quadrature nodes (ρ^{cyl},φ,z) on the cylinder with radius 1 that goes from $z=-1$ to $z=1$ with the required rotation angles (α,β,γ) to rotate a node to its representative symmetric node (identified with (0,0,0) angles), for which quadrature weight table is given. Convert the nodes from cylindrical to Cartesian coordinates before using them with the weights.

Index	ρ^{cyl}	φ	z	α	β	γ	Index	ρ^{cyl}	φ	z	α	β	γ
1	$(5-\sqrt{15})/10$	$\pi/6$	$-\sqrt{3/5}$	0	π	$2\pi/3$	28	$1/2$	$7\pi/6$	$-\sqrt{3/5}$	0	π	$-\pi/3$
2	$(5-\sqrt{15})/10$	$\pi/6$	0	0	0	0	29	$1/2$	$7\pi/6$	0	0	0	π
3	$(5-\sqrt{15})/10$	$\pi/6$	$\sqrt{3/5}$	0	0	0	30	$1/2$	$7\pi/6$	$\sqrt{3/5}$	0	0	π
4	$(5-\sqrt{15})/10$	$\pi/2$	$-\sqrt{3/5}$	0	π	$\pi/3$	31	$1/2$	$3\pi/2$	$-\sqrt{3/5}$	0	π	$-2\pi/3$
5	$(5-\sqrt{15})/10$	$\pi/2$	0	0	0	$\pi/3$	32	$1/2$	$3\pi/2$	0	0	0	$-2\pi/3$
6	$(5-\sqrt{15})/10$	$\pi/2$	$\sqrt{3/5}$	0	0	$\pi/3$	33	$1/2$	$3\pi/2$	$\sqrt{3/5}$	0	0	$-2\pi/3$
7	$(5-\sqrt{15})/10$	$5\pi/6$	$-\sqrt{3/5}$	0	π	0	34	$1/2$	$11\pi/6$	$-\sqrt{3/5}$	0	π	π
8	$(5-\sqrt{15})/10$	$5\pi/6$	0	0	0	$2\pi/3$	35	$1/2$	$11\pi/6$	0	0	0	$-\pi/3$
9	$(5-\sqrt{15})/10$	$5\pi/6$	$\sqrt{3/5}$	0	0	$2\pi/3$	36	$1/2$	$11\pi/6$	$\sqrt{3/5}$	0	0	$-\pi/3$
10	$(5-\sqrt{15})/10$	$7\pi/6$	$-\sqrt{3/5}$	0	π	$-\pi/3$	37	$(5+\sqrt{15})/10$	$\pi/6$	$-\sqrt{3/5}$	0	π	$2\pi/3$
11	$(5-\sqrt{15})/10$	$7\pi/6$	0	0	0	π	38	$(5+\sqrt{15})/10$	$\pi/6$	0	0	0	0
12	$(5-\sqrt{15})/10$	$7\pi/6$	$\sqrt{3/5}$	0	0	π	39	$(5+\sqrt{15})/10$	$\pi/6$	$\sqrt{3/5}$	0	0	0
13	$(5-\sqrt{15})/10$	$3\pi/2$	$-\sqrt{3/5}$	0	π	$-2\pi/3$	40	$(5+\sqrt{15})/10$	$\pi/2$	$-\sqrt{3/5}$	0	π	$\pi/3$
14	$(5-\sqrt{15})/10$	$3\pi/2$	0	0	0	$-2\pi/3$	41	$(5+\sqrt{15})/10$	$\pi/2$	0	0	0	$\pi/3$
15	$(5-\sqrt{15})/10$	$3\pi/2$	$\sqrt{3/5}$	0	0	$-2\pi/3$	42	$(5+\sqrt{15})/10$	$\pi/2$	$\sqrt{3/5}$	0	0	$\pi/3$
16	$(5-\sqrt{15})/10$	$11\pi/6$	$-\sqrt{3/5}$	0	π	π	43	$(5+\sqrt{15})/10$	$5\pi/6$	$-\sqrt{3/5}$	0	π	0
17	$(5-\sqrt{15})/10$	$11\pi/6$	0	0	0	$-\pi/3$	44	$(5+\sqrt{15})/10$	$5\pi/6$	0	0	0	$2\pi/3$
18	$(5-\sqrt{15})/10$	$11\pi/6$	$\sqrt{3/5}$	0	0	$-\pi/3$	45	$(5+\sqrt{15})/10$	$5\pi/6$	$\sqrt{3/5}$	0	0	$2\pi/3$
19	$1/2$	$\pi/6$	$-\sqrt{3/5}$	0	π	$2\pi/3$	46	$(5+\sqrt{15})/10$	$7\pi/6$	$-\sqrt{3/5}$	0	π	$-\pi/3$
20	$1/2$	$\pi/6$	0	0	0	0	47	$(5+\sqrt{15})/10$	$7\pi/6$	0	0	0	π
21	$1/2$	$\pi/6$	$\sqrt{3/5}$	0	0	0	48	$(5+\sqrt{15})/10$	$7\pi/6$	$\sqrt{3/5}$	0	0	π
22	$1/2$	$\pi/2$	$-\sqrt{3/5}$	0	π	$\pi/3$	49	$(5+\sqrt{15})/10$	$3\pi/2$	$-\sqrt{3/5}$	0	π	$-2\pi/3$
23	$1/2$	$\pi/2$	0	0	0	$\pi/3$	50	$(5+\sqrt{15})/10$	$3\pi/2$	0	0	0	$-2\pi/3$
24	$1/2$	$\pi/2$	$\sqrt{3/5}$	0	0	$\pi/3$	51	$(5+\sqrt{15})/10$	$3\pi/2$	$\sqrt{3/5}$	0	0	$-2\pi/3$
25	$1/2$	$5\pi/6$	$-\sqrt{3/5}$	0	π	0	52	$(5+\sqrt{15})/10$	$11\pi/6$	$-\sqrt{3/5}$	0	π	π
26	$1/2$	$5\pi/6$	0	0	0	$2\pi/3$	53	$(5+\sqrt{15})/10$	$11\pi/6$	0	0	0	$-\pi/3$
27	$1/2$	$5\pi/6$	$\sqrt{3/5}$	0	0	$2\pi/3$	54	$(5+\sqrt{15})/10$	$11\pi/6$	$\sqrt{3/5}$	0	0	$-\pi/3$

Table 7: Weights for when the singularity is at $((5-\sqrt{15})/10,\pi/6,0)$. After a rotation, this table can be used when the singularity at index 2, 5, 8, 11, 14, or 17: on the inner red ($z=0$) circle in Fig. 5. $\delta_0=0$ and $\delta_1=(5-\sqrt{15})/20$.

Index	$1/R,\delta_0$	$1/R^2,\delta_0$	$1/R^2,\delta_1$	$1/R^3,\delta_1$	Index	$1/R,\delta_0$	$1/R^2,\delta_0$	$1/R^2,\delta_1$	$1/R^3,\delta_1$
1	0.02791092	0.05191174	0.05198659	0.13260777	28	0.13526561	0.14640650	0.14623280	0.16548926
2	0.17564191	1.72872594	1.05320514	9.16458216	29	0.32422056	0.52010710	0.52097126	0.87295679
3	0.02791092	0.05191174	0.05198659	0.13260777	30	0.13526561	0.14640650	0.14623280	0.16548926
4	0.02685134	0.04585813	0.04585445	0.09708571	31	0.13950318	0.15655562	0.15699932	0.18481939
5	0.12838217	0.64961989	0.63461234	3.91751248	32	0.34507384	0.57773822	0.58673798	0.97686626
6	0.02685134	0.04585813	0.04585445	0.09708571	33	0.13950318	0.15655562	0.15699932	0.18481939
7	0.02507754	0.03859513	0.03878762	0.06744157	34	0.15170547	0.18782963	0.18778562	0.25177656
8	0.09337518	0.29441181	0.31084814	0.96907564	35	0.42180110	0.91892500	0.91514780	2.22353478
9	0.02507754	0.03859513	0.03878762	0.06744157	36	0.15170547	0.18782963	0.18778562	0.25177656
10	0.02514933	0.03769554	0.03810122	0.06393314	37	0.13368287	0.12559468	0.12562579	0.11582178
11	0.09075834	0.29724958	0.29087543	1.13030477	38	0.28021623	0.29166363	0.29215271	−0.00359112
12	0.02514933	0.03769554	0.03810122	0.06393314	39	0.13368287	0.12559468	0.12562579	0.11582178
13	0.02654590	0.04086847	0.03986984	0.06898660	40	0.12800665	0.11508226	0.11508534	0.10252984
14	0.09908123	0.32691738	0.31234313	0.97647352	41	0.26337438	0.27904304	0.27954071	0.21187152
15	0.02654590	0.04086847	0.03986984	0.06898660	42	0.12800665	0.11508226	0.11508534	0.10252984
16	0.02639704	0.04529969	0.04540352	0.09649951	43	0.11847768	0.09829615	0.09831798	0.08119290
17	0.12768001	0.64441192	0.63499195	3.92114939	44	0.23503210	0.23203674	0.23327975	0.22438597
18	0.02639704	0.04529969	0.04540352	0.09649951	45	0.11847768	0.09829615	0.09831798	0.08119290
19	0.15864936	0.20872220	0.20860981	0.30624590	46	0.11460326	0.09190689	0.09195545	0.07340865
20	0.48299618	1.27819180	1.27457629	4.29092632	47	0.22417061	0.21202517	0.21178186	0.18600352
21	0.15864936	0.20872220	0.20860981	0.30624590	48	0.11460326	0.09190689	0.09195545	0.07340865
22	0.15152729	0.18761865	0.18760866	0.25154883	49	0.11865550	0.09857157	0.09844688	0.08137727
23	0.42158368	0.91711250	0.91533397	2.22520946	50	0.23572430	0.23598963	0.23346474	0.22531414
24	0.15152729	0.18761865	0.18760866	0.25154883	51	0.11865550	0.09857157	0.09844688	0.08137727
25	0.14013800	0.15753883	0.15746043	0.18547876	52	0.12795734	0.11502417	0.11503636	0.10246691
26	0.34754456	0.59184332	0.58739662	0.98016538	53	0.26331637	0.27854988	0.27959367	0.21234453
27	0.14013800	0.15753883	0.15746043	0.18547876	54	0.12795734	0.11502417	0.11503636	0.10246691

Table 8: Weights for when the singularity is at $(1/2,\pi/6,0)$. After a rotation, this table can be used when the singularity is at index 20, 23, 26, 29, 32, or 35: on the middle red ($z=0$) circle in Fig. 5. $\delta_0=0$ and $\delta_1=(5-\sqrt{15})/20$.

Index	$1/R,\delta_0$	$1/R^2,\delta_0$	$1/R^2,\delta_1$	$1/R^3,\delta_1$	Index	$1/R,\delta_0$	$1/R^2,\delta_0$	$1/R^2,\delta_1$	$1/R^3,\delta_1$
1	0.02283933	0.03091841	0.03092921	0.04696740	28	0.10413423	0.08653936	0.08653422	0.07693692
2	0.07221363	0.19710851	0.19664418	0.63276141	29	0.21343938	0.25301974	0.25275158	0.43014911
3	0.02283933	0.03091841	0.03092921	0.04696740	30	0.10413423	0.08653936	0.08653422	0.07693692
4	0.02193686	0.02779612	0.02774341	0.03762823	31	0.11212231	0.09665933	0.09665830	0.07989260
5	0.06187675	0.13298485	0.13277766	0.29834264	32	0.22257727	0.19942886	0.19975488	0.00049664
6	0.02193686	0.02779612	0.02774341	0.03762823	33	0.11212231	0.09665933	0.09665830	0.07989260
7	0.01965209	0.02184505	0.02187945	0.02473750	34	0.14764344	0.17809604	0.17809805	0.23279630
8	0.04724143	0.07356360	0.07369672	0.10690412	35	0.40014812	0.84116287	0.84017780	2.07787301
9	0.01965209	0.02184505	0.02187945	0.02473750	36	0.14764344	0.17809604	0.17809805	0.23279630
10	0.01909389	0.02024715	0.02025727	0.02197053	37	0.17471005	0.22425094	0.22425161	0.30969581
11	0.04444496	0.06673861	0.06677998	0.10399176	38	0.50209678	1.13892606	1.13777708	2.88834973
12	0.01909389	0.02024715	0.02025727	0.02197053	39	0.17471005	0.22425094	0.22425161	0.30969581
13	0.01973505	0.02194441	0.02194776	0.02482378	40	0.13608049	0.13363116	0.13362486	0.13716442
14	0.04745866	0.07396799	0.07398143	0.10744288	41	0.30354112	0.41963774	0.41961212	0.62050260
15	0.01973505	0.02194441	0.02194776	0.02482378	42	0.13608049	0.13363116	0.13362486	0.13716442
16	0.02171451	0.02753172	0.02752534	0.03735703	43	0.09906250	0.06714067	0.06714471	0.04299581
17	0.06129888	0.13192297	0.13189590	0.29671491	44	0.18018891	0.12649446	0.12651047	0.05431074
18	0.02171451	0.02753172	0.02752534	0.03735703	45	0.09906250	0.06714067	0.06714471	0.04299581
19	0.18496981	0.29886171	0.29865072	0.58898802	46	0.09136521	0.05948664	0.05948808	0.04071871
20	0.80708944	4.22624713	3.52176269	21.11116609	47	0.16897155	0.13414784	0.13415342	0.12930034
21	0.18496981	0.29886171	0.29865072	0.58898802	48	0.09136521	0.05948664	0.05948808	0.04071871
22	0.14754517	0.17797919	0.17800137	0.23267604	49	0.09907242	0.06715256	0.06715288	0.04300614
23	0.39989273	0.84069352	0.83978749	2.07715256	50	0.18021490	0.12654290	0.12654440	0.05437501
24	0.14754517	0.17797919	0.17800137	0.23267604	51	0.09907242	0.06715256	0.06715288	0.04300614
25	0.11215777	0.09670181	0.09668748	0.07992953	52	0.13605288	0.13359832	0.13359768	0.13713061
26	0.22267015	0.19960191	0.19987615	0.00072635	53	0.30346935	0.41950585	0.41950242	0.62030010
27	0.11215777	0.09670181	0.09668748	0.07992953	54	0.13605288	0.13359832	0.13359768	0.13713061

Table 9: Weights for when the singularity is at $((5+\sqrt{15})/10,\pi/6,0)$. After a rotation, this table can be used when the singularity is at index 38, 41, 44, 47, 50, or 53: on the outer red ($z=0$) circle in Fig. 5. $\delta_0=0$ and $\delta_1=(5-\sqrt{15})/20$.

Index	$1/R,\delta_0$	$1/R^2,\delta_0$	$1/R^2,\delta_1$	$1/R^3,\delta_1$	Index	$1/R,\delta_0$	$1/R^2,\delta_0$	$1/R^2,\delta_1$	$1/R^3,\delta_1$
1	0.01653280	0.01367508	0.01357085	0.00845805	28	0.08239787	0.05403767	0.05410443	0.03762349
2	0.02934041	0.01042251	0.00913333	−0.03072137	29	0.15299348	0.12350255	0.12367587	0.12226323
3	0.01653280	0.01367508	0.01357085	0.00845805	30	0.08239787	0.05403767	0.05410443	0.03762349
4	0.01592194	0.01426866	0.01494815	0.01331480	31	0.08931856	0.06060919	0.06060449	0.03909863
5	0.03278013	0.03566008	0.03740818	0.03581580	32	0.16278183	0.11546130	0.11544796	0.05237935
6	0.01592194	0.01426866	0.01494815	0.01331480	33	0.08931856	0.06060919	0.06060449	0.03909863
7	0.01522598	0.01278044	0.01230476	0.01046091	34	0.12238222	0.11967182	0.11966137	0.12237014
8	0.03063342	0.03217883	0.03096536	0.03370042	35	0.27231945	0.37526321	0.37523662	0.55770994
9	0.01522598	0.01278044	0.01230476	0.01046091	36	0.12238222	0.11967182	0.11966137	0.12237014
10	0.01482078	0.01178493	0.01165189	0.00919770	37	0.19634196	0.29732176	0.29710621	0.54919938
11	0.02889755	0.02716477	0.02681760	0.02362016	38	0.78066629	3.91216510	3.20356192	19.61718225
12	0.01482078	0.01178493	0.01165189	0.00919770	39	0.19634196	0.29732176	0.29710621	0.54919938
13	0.01492096	0.01252035	0.01251950	0.01065345	40	0.12805642	0.12110134	0.12118071	0.12465180
14	0.03001634	0.03152497	0.03152602	0.03432550	41	0.28468672	0.40939799	0.40928543	0.75633239
15	0.01492096	0.01252035	0.01251950	0.01065345	42	0.12805642	0.12110134	0.12118071	0.12465180
16	0.01601139	0.01434205	0.01438296	0.01281160	43	0.08155056	0.04330596	0.04325146	0.01743879
17	0.03295751	0.03583700	0.03594218	0.03419652	44	0.13662999	0.05022311	0.05018956	−0.08650883
18	0.01601139	0.01434205	0.01438296	0.01281160	45	0.08155056	0.04330596	0.04325146	0.01743879
19	0.15816527	0.20524373	0.20527178	0.28892326	46	0.07582144	0.04264306	0.04262406	0.02820478
20	0.46312490	1.07803340	1.08049751	2.68117237	47	0.13811704	0.10658176	0.10645337	0.15061330
21	0.15816527	0.20524373	0.20527178	0.28892326	48	0.07582144	0.04264306	0.04262406	0.02820478
22	0.12241694	0.11970019	0.11941550	0.12215128	49	0.08151367	0.04327448	0.04327599	0.01746078
23	0.27238815	0.37533129	0.37459899	0.55700584	50	0.13655533	0.05014392	0.05025360	−0.08643742
24	0.12241694	0.11970019	0.11941550	0.12215128	51	0.08151367	0.04327448	0.04327599	0.01746078
25	0.08918683	0.06049679	0.06069257	0.03917761	52	0.12806602	0.12110918	0.12111178	0.12459044
26	0.16251524	0.11517856	0.11567794	0.05263578	53	0.28470571	0.40941680	0.40910667	0.75613500
27	0.08918683	0.06049679	0.06069257	0.03917761	54	0.12806602	0.12110918	0.12111178	0.12459044

Table 10: Weights for when the singularity is at $((5-\sqrt{15})/10,\pi/6,\sqrt{3/5})$. After a rotation, this table can be used when the singularity is at index 1, 3, 4, 6, 7, 9, 10, 12, 13, 15, 16, or 18: on the inner green ($z=\sqrt{3/5}$) or blue ($z=-\sqrt{3/5}$) circle in Fig. 5. $\delta_0=0$ and $\delta_1=(5-\sqrt{15})/20$.

Index	$1/R,\delta_0$	$1/R^2,\delta_0$	$1/R^2,\delta_1$	$1/R^3,\delta_1$	Index	$1/R,\delta_0$	$1/R^2,\delta_0$	$1/R^2,\delta_1$	$1/R^3,\delta_1$
1	0.01072087	0.00588255	0.00567940	0.02193820	28	0.07513969	0.03968675	0.03968134	0.01438157
2	0.04543787	0.07890642	0.07934895	0.12422889	29	0.21753680	0.23986099	0.23973742	0.27991765
3	0.14387648	1.64515230	0.96942295	8.98931498	30	0.21160191	0.35741080	0.35715645	0.63101323
4	0.01054445	0.00446095	0.00449385	0.00475310	31	0.07558546	0.03940987	0.03938776	0.01212602
5	0.04360662	0.07437572	0.07467865	0.13256796	32	0.22537452	0.25874389	0.25827940	0.31555093
6	0.09764226	0.56935910	0.55710657	3.73282913	33	0.22727169	0.40533380	0.40354244	0.69105357
7	0.01073744	0.00430075	0.00424374	−0.00198418	34	0.07618107	0.03795025	0.03796672	0.00671875
8	0.04197098	0.06695582	0.06572170	0.11434873	35	0.24482261	0.31124682	0.31143489	0.42925719
9	0.06901262	0.24493030	0.24638074	0.81855373	36	0.28340910	0.67013754	0.67276840	1.78832730
10	0.01075264	0.00455966	0.00457239	−0.00077616	37	0.08132738	0.04403006	0.04402968	0.02033293
11	0.04093187	0.06315041	0.06347652	0.10547563	38	0.21393564	0.20276278	0.20276921	0.19352884
12	0.06421796	0.23715574	0.23349189	1.00798990	39	0.17722367	0.17278230	0.17330603	−0.13266767
13	0.01068216	0.00427194	0.00432358	−0.00209693	40	0.08026280	0.04340839	0.04341277	0.02155613
14	0.04174836	0.06658319	0.06761312	0.11808304	41	0.20460001	0.18476302	0.18479190	0.16688416
15	0.06842130	0.24072553	0.25070136	0.83865595	42	0.16673990	0.17381650	0.17456576	0.10405969
16	0.01074596	0.00456345	0.00451944	0.00474217	43	0.07817692	0.04173747	0.04173066	0.02150047
17	0.04441746	0.07573338	0.07529152	0.13380122	44	0.18928423	0.15719926	0.15705616	0.12966869
18	0.09973916	0.58371506	0.55906611	3.74392191	45	0.14890939	0.14925104	0.14875113	0.14536761
19	0.07640474	0.03693288	0.03693365	0.00593467	46	0.07713565	0.04077747	0.04077896	0.02090275
20	0.25720568	0.34721548	0.34719402	0.50921671	47	0.18293449	0.14665194	0.14668601	0.11715599
21	0.33322331	0.99237583	0.98862902	3.73962869	48	0.14159581	0.13465994	0.13472821	0.11741371
22	0.07626912	0.03799501	0.03797924	0.00671201	49	0.07817076	0.04173425	0.04174046	0.02148675
23	0.24517689	0.31184002	0.31173464	0.42985923	50	0.18925942	0.15715774	0.15728844	0.13012735
24	0.28432481	0.67640183	0.67369511	1.79349948	51	0.14884340	0.14878093	0.14928510	0.14786175
25	0.07556328	0.03939829	0.03942272	0.01207707	52	0.08028750	0.04342095	0.04341633	0.02155418
26	0.22528517	0.25859434	0.25910744	0.31718599	53	0.20469940	0.18492943	0.18487706	0.16705515
27	0.22703407	0.40364140	0.40544444	0.69993358	54	0.16699677	0.17557353	0.17482812	0.10552179

Table 11: Weights for when the singularity is at $(1/2,\pi/6,\sqrt{3/5})$. After a rotation, this table can be used when the singularity is at index 19, 21, 22, 23, 25, 27, 28, 30, 31, 33, 34, or 36: on the middle green ($z=\sqrt{3/5}$) or blue ($z=-\sqrt{3/5}$) circle in Fig. 5. $\delta_0=0$ and $\delta_1=(5-\sqrt{15})/20$.

Index	$1/R,\delta_0$	$1/R^2,\delta_0$	$1/R^2,\delta_1$	$1/R^3,\delta_1$	Index	$1/R,\delta_0$	$1/R^2,\delta_0$	$1/R^2,\delta_1$	$1/R^3,\delta_1$
1	0.01063698	0.00493586	0.00502486	$8.61712498\cdot10^{-5}$	28	0.06933499	0.03607900	0.03605656	0.01734472
2	0.03668696	0.05126789	0.05192827	0.07963748	29	0.16659034	0.13921113	0.13904625	0.12463261
3	0.04971647	0.15219044	0.15278600	0.54422098	30	0.13691565	0.17386722	0.17334429	0.33889500
4	0.01098100	0.00533149	0.00519237	0.00042817	31	0.07192033	0.03899138	0.03899376	0.01996522
5	0.03613689	0.04715035	0.04613419	0.06500611	32	0.17905664	0.15460262	0.15462204	0.12943217
6	0.04223421	0.09749629	0.09581657	0.23149876	33	0.13975814	0.11629336	0.11666109	−0.07207833
7	0.01057689	0.00562301	0.00565096	0.00205010	34	0.07591247	0.03831224	0.03832300	0.00878000
8	0.03151317	0.03565129	0.03584509	0.04176742	35	0.23842667	0.29488510	0.29496515	0.39530256
9	0.03056397	0.04906280	0.04936825	0.07232703	36	0.26827146	0.61661899	0.61575214	1.68705053
10	0.01063116	0.00575284	0.00580472	0.00243352	37	0.08496541	0.04144310	0.04145318	0.00443000
11	0.03042716	0.03267545	0.03305922	0.03669576	38	0.28300701	0.37392764	0.37400580	0.53117979
12	0.02856263	0.04470675	0.04534703	0.07479749	39	0.33967482	0.84103106	0.84000632	2.34267464
13	0.01064869	0.00565970	0.00565477	0.00205031	40	0.08119660	0.04319378	0.04317666	0.01869591
14	0.03173746	0.03592354	0.03587993	0.04181639	41	0.21824222	0.21701663	0.21689149	0.22806428
15	0.03080107	0.04951875	0.04943619	0.07247462	42	0.19585505	0.28255711	0.28234953	0.44033974
16	0.01072191	0.00519902	0.00517219	0.00042399	43	0.07255353	0.03665220	0.03665551	0.01877686
17	0.03532825	0.04616992	0.04597800	0.06480153	44	0.15795398	0.10640687	0.10642984	0.06704786
18	0.04138046	0.09585790	0.09554543	0.23096131	45	0.11284792	0.07749212	0.07752860	0.02523576
19	0.07637200	0.03375436	0.03350979	0.02687263	46	0.06875441	0.03261720	0.03262347	0.01492906
20	0.30227422	0.49041671	0.49055374	0.83138185	47	0.14593107	0.09516357	0.09520977	0.06589262
21	0.60844212	3.74971183	3.04415733	20.04252076	48	0.10663603	0.08695461	0.08703134	0.08951377
22	0.07579747	0.03825343	0.03831409	0.00877814	49	0.07256209	0.03665658	0.03665594	0.01877688
23	0.23806774	0.29444992	0.29489626	0.39521237	50	0.15798072	0.10643933	0.10643380	0.06705345
24	0.26789251	0.61589179	0.61563264	1.68681386	51	0.11287619	0.07754648	0.07753638	0.02525277
25	0.07195092	0.03900702	0.03899529	0.01996529	52	0.08116427	0.04317725	0.04317416	0.01869539
26	0.17915222	0.15471863	0.15463627	0.12945225	53	0.21814130	0.21689428	0.21687214	0.22803895
27	0.13985918	0.11648766	0.11668903	−0.07201731	54	0.19574850	0.28235265	0.28231597	0.44027327

Table 12: Weights for when the singularity is at $((5+\sqrt{15})/10,\pi/6,\sqrt{3/5})$. After a rotation, this table can be used when the singularity is at index 37, 39, 40, 42, 43, 45, 46, 48, 49, 51, 52, 53, or 54: on the outer green ($z=\sqrt{3/5}$) or blue ($z=-\sqrt{3/5}$) circle in Fig. 5. $\delta_0=0$ and $\delta_1=(5-\sqrt{15})/20$.

Index	$1/R,\delta_0$	$1/R^2,\delta_0$	$1/R^2,\delta_1$	$1/R^3,\delta_1$	Index	$1/R,\delta_0$	$1/R^2,\delta_0$	$1/R^2,\delta_1$	$1/R^3,\delta_1$
1	0.01058741	0.00605595	0.00601660	0.00383822	28	0.06185368	0.02928838	0.02931437	0.01334518
2	0.02630517	0.02141959	0.02125327	0.01204361	29	0.13164814	0.08652372	0.08663088	0.06094551
3	0.01759198	0.00136738	0.00017345	−0.02852274	30	0.09663098	0.08024833	0.08036092	0.08481176
4	0.01000575	0.00542958	0.00569731	0.00288167	31	0.06542012	0.03297844	0.03297683	0.01679421
5	0.02544531	0.02287697	0.02396704	0.02151456	32	0.14244522	0.09613538	0.09612781	0.06115405
6	0.02080273	0.02273951	0.02387339	0.02195153	33	0.10200014	0.07092132	0.07091252	0.02510320
7	0.00999957	0.00532189	0.00513212	0.00257149	34	0.07322032	0.03898346	0.03897940	0.01698651
8	0.02432404	0.02047370	0.01971094	0.01690348	35	0.19618249	0.19419005	0.19417329	0.20332746
9	0.01945719	0.02091056	0.02012425	0.02271652	36	0.17562420	0.25279426	0.25277716	0.39745496
10	0.01002419	0.00530585	0.00525450	0.00268841	37	0.08563200	0.04107773	0.04086669	0.03440879
11	0.02365889	0.01881373	0.01860015	0.01472465	38	0.31934326	0.48466629	0.48507187	0.76552597
12	0.01826277	0.01731645	0.01709083	0.01492436	39	0.57966971	3.46630540	2.75708344	18.68149505
13	0.00980126	0.00521590	0.00521490	0.00261259	40	0.07898186	0.04108709	0.04111829	0.01758517
14	0.02383673	0.02005694	0.02005568	0.01721595	41	0.20531342	0.19667588	0.19680358	0.20664337
15	0.01906532	0.02048763	0.02048861	0.02313153	42	0.18455356	0.28448713	0.28430241	0.58620724
16	0.01006522	0.00546118	0.00547720	0.00277219	43	0.06567192	0.03033435	0.03031263	0.01466593
17	0.02558815	0.02299432	0.02305996	0.02069850	44	0.12999965	0.06819199	0.06810447	0.02602445
18	0.02091511	0.02285331	0.02292144	0.02087764	45	0.08453210	0.02500229	0.02501783	−0.08568947
19	0.07645779	0.03690778	0.03691848	0.00246778	46	0.06085274	0.02551540	0.02550798	0.01009651
20	0.25640456	0.34280943	0.34285181	0.49721435	47	0.12127783	0.06859311	0.06856271	0.04615874
21	0.31497705	0.80087806	0.80331881	2.15839025	48	0.08748948	0.07209927	0.07198806	0.11839108
22	0.07324345	0.03899574	0.03888362	0.01693887	49	0.06564795	0.03032153	0.03032208	0.01467062
23	0.19623792	0.19423540	0.19377869	0.20297253	50	0.12994071	0.06814155	0.06814384	0.02606014
24	0.17566771	0.25283803	0.25236313	0.39698802	51	0.08448468	0.02495107	0.02505945	−0.08564206
25	0.06533450	0.03293268	0.03301078	0.01681106	52	0.07898826	0.04109049	0.04109143	0.01757182
26	0.14223475	0.09595528	0.09626921	0.06128222	53	0.20532875	0.19668842	0.19669295	0.20654387
27	0.10183083	0.07073843	0.07106198	0.02527346	54	0.18456559	0.28449922	0.28418633	0.58607634

force quadrature parameters n, n_{cyl}, and n_w.The code is allowed to subdivide the cylinder further in all cases.

Finally, the size δ of the exclusion volume V_δ is specified in the tables as either $\delta_0 = 0$ or $\delta_1 = (5-\sqrt{15})/20$, which is the half of the smallest distance for the quadrature nodes to the cylindrical boundary of the cylinder.

Note that the weights are given for points in Cartesian coordinates. Since the weights contain the Jacobian for the transformation from cylindrical to Cartesian coordinates, convert the nodes to Cartesian coordinates according to the mapping

$$(\rho^{cyl},\phi,z) \mapsto (\rho^{cyl}\cos(\phi),\rho^{cyl}\sin(\phi),z) \tag{C.1}$$

before using them with the tables of weights.

D Integration quadrature nodes and weights for singular kernels over a sphere

We provide the quadrature nodes (also the interpolation nodes) and weights for integrating over a sphere with radius 1 according to Eq. (2.4) when $M = 42$ and the singularity corresponds to a quadrature node. The six cases for the weights correspond to when $\theta = 0$ or $\pi/3$ and all values for ρ. When the singularity is at a quadrature node that we do not list, the corresponding weights can be obtained by rotating the sphere in Fig. 6 around the x, y, and z axes by α, β, and γ, respectively.

Table 13: Quadrature nodes (ρ,φ,θ) on the sphere with radius 1 with the required rotation angles (α,β,γ) to rotate a node to its representative symmetric node (identified with (0,0,0) angles), for which quadrature weight table is given. Convert the points from spherical to Cartesian coordinates before using them with the weights.

INDEX	ρ	φ	θ	α	β	γ	INDEX	ρ	φ	θ	α	β	γ
1	$(5-\sqrt{15})/10$	0	0	0	0	0	22	$1/2$	0	$2\pi/3$	0	π	π
2	$(5-\sqrt{15})/10$	0	$\pi/3$	0	0	0	23	$1/2$	$\pi/3$	$2\pi/3$	0	π	$2\pi/3$
3	$(5-\sqrt{15})/10$	$\pi/3$	$\pi/3$	0	0	$\pi/3$	24	$1/2$	$2\pi/3$	$2\pi/3$	0	π	$\pi/3$
4	$(5-\sqrt{15})/10$	$2\pi/3$	$\pi/3$	0	0	$2\pi/3$	25	$1/2$	π	$2\pi/3$	0	π	0
5	$(5-\sqrt{15})/10$	π	$\pi/3$	0	0	π	26	$1/2$	$4\pi/3$	$2\pi/3$	0	π	$-\pi/3$
6	$(5-\sqrt{15})/10$	$4\pi/3$	$\pi/3$	0	0	$-2\pi/3$	27	$1/2$	$5\pi/3$	$2\pi/3$	0	π	$-2\pi/3$
7	$(5-\sqrt{15})/10$	$5\pi/3$	$\pi/3$	0	0	$-\pi/3$	28	$1/2$	0	π	0	π	0
8	$(5-\sqrt{15})/10$	0	$2\pi/3$	0	π	π	29	$(5+\sqrt{15})/10$	0	0	0	0	0
9	$(5-\sqrt{15})/10$	$\pi/3$	$2\pi/3$	0	π	$2\pi/3$	30	$(5+\sqrt{15})/10$	0	$\pi/3$	0	0	0
10	$(5-\sqrt{15})/10$	$2\pi/3$	$2\pi/3$	0	π	$\pi/3$	31	$(5+\sqrt{15})/10$	$\pi/3$	$\pi/3$	0	0	$\pi/3$
11	$(5-\sqrt{15})/10$	π	$2\pi/3$	0	π	0	32	$(5+\sqrt{15})/10$	$2\pi/3$	$\pi/3$	0	0	$2\pi/3$
12	$(5-\sqrt{15})/10$	$4\pi/3$	$2\pi/3$	0	π	$-\pi/3$	33	$(5+\sqrt{15})/10$	π	$\pi/3$	0	0	π
13	$(5-\sqrt{15})/10$	$5\pi/3$	$2\pi/3$	0	π	$-2\pi/3$	34	$(5+\sqrt{15})/10$	$4\pi/3$	$\pi/3$	0	0	$-2\pi/3$
14	$(5-\sqrt{15})/10$	0	π	0	π	0	35	$(5+\sqrt{15})/10$	$5\pi/3$	$\pi/3$	0	0	$-\pi/3$
15	$1/2$	0	0	0	0	0	36	$(5+\sqrt{15})/10$	0	$2\pi/3$	0	π	π
16	$1/2$	0	$\pi/3$	0	0	0	37	$(5+\sqrt{15})/10$	$\pi/3$	$2\pi/3$	0	π	$2\pi/3$
17	$1/2$	$\pi/3$	$\pi/3$	0	0	$\pi/3$	38	$(5+\sqrt{15})/10$	$2\pi/3$	$2\pi/3$	0	π	$\pi/3$
18	$1/2$	$2\pi/3$	$\pi/3$	0	0	$2\pi/3$	39	$(5+\sqrt{15})/10$	π	$2\pi/3$	0	π	0
19	$1/2$	π	$\pi/3$	0	0	π	40	$(5+\sqrt{15})/10$	$4\pi/3$	$2\pi/3$	0	π	$-\pi/3$
20	$1/2$	$4\pi/3$	$\pi/3$	0	0	$-2\pi/3$	41	$(5+\sqrt{15})/10$	$5\pi/3$	$2\pi/3$	0	π	$-2\pi/3$
21	$1/2$	$5\pi/3$	$\pi/3$	0	0	$-\pi/3$	42	$(5+\sqrt{15})/10$	0	π	0	π	0

Table 14: Weights for when the singularity is at $((5-\sqrt{15})/10,0,0)$. After a rotation, this table can be used when the singularity is at index 1 or 14: at the inner point on either line in Fig. 6. $\delta_0=0$ and $\delta_1=(5-\sqrt{15})/20$.

Index	$1/R,\delta_0$	$1/R^2,\delta_0$	$1/R^2,\delta_1$	$1/R^3,\delta_1$	Index	$1/R,\delta_0$	$1/R^2,\delta_0$	$1/R^2,\delta_1$	$1/R^3,\delta_1$
1	0.05686930	1.09792933	0.45670400	5.20917399	22	0.18549010	0.34193235	0.34193582	0.64775546
2	0.03011260	0.22386604	0.21167602	1.60566417	23	0.18549010	0.34193235	0.34193582	0.64775546
3	0.03011260	0.22386604	0.21167602	1.60566417	24	0.18549010	0.34193235	0.34193582	0.64775546
4	0.03011260	0.22386604	0.21167602	1.60566417	25	0.18549010	0.34193235	0.34193582	0.64775546
5	0.03011260	0.22386604	0.21167602	1.60566417	26	0.18549010	0.34193235	0.34193582	0.64775546
6	0.03011260	0.22386604	0.21167602	1.60566417	27	0.18549010	0.34193235	0.34193582	0.64775546
7	0.03011260	0.22386604	0.21167602	1.60566417	28	0.11713084	0.18238616	0.18237805	0.33274142
8	0.01865685	0.07869126	0.08240042	0.29300825	29	0.20509752	0.23669049	0.23878158	−0.02381104
9	0.01865685	0.07869126	0.08240042	0.29300825	30	0.23995075	0.27234988	0.27233864	0.24502604
10	0.01865685	0.07869126	0.08240042	0.29300825	31	0.23995075	0.27234988	0.27233864	0.24502604
11	0.01865685	0.07869126	0.08240042	0.29300825	32	0.23995075	0.27234988	0.27233864	0.24502604
12	0.01865685	0.07869126	0.08240042	0.29300825	33	0.23995075	0.27234988	0.27233864	0.24502604
13	0.01865685	0.07869126	0.08240042	0.29300825	34	0.23995075	0.27234988	0.27233864	0.24502604
14	0.01117095	0.05632839	0.04806652	0.32827946	35	0.23995075	0.27234988	0.27233864	0.24502604
15	0.22668260	0.76934167	0.75946212	3.35429076	36	0.21738927	0.22935874	0.22936018	0.23305432
16	0.22403161	0.52608151	0.52609563	1.43338189	37	0.21738927	0.22935874	0.22936018	0.23305432
17	0.22403161	0.52608151	0.52609563	1.43338189	38	0.21738927	0.22935874	0.22936018	0.23305432
18	0.22403161	0.52608151	0.52609563	1.43338189	39	0.21738927	0.22935874	0.22936018	0.23305432
19	0.22403161	0.52608151	0.52609563	1.43338189	40	0.21738927	0.22935874	0.22936018	0.23305432
20	0.22403161	0.52608151	0.52609563	1.43338189	41	0.21738927	0.22935874	0.22936018	0.23305432
21	0.22403161	0.52608151	0.52609563	1.43338189	42	0.14584464	0.13667536	0.13667222	0.11453720

Table 15: Weights for when the singularity is at $(1/2,0,0)$. After a rotation, this table can be used when the singularity is at index 15 or 28: at the middle point on either line in Fig. 6. $\delta_0=0$ and $\delta_1=(5-\sqrt{15})/20$.

Index	$1/R,\delta_0$	$1/R^2,\delta_0$	$1/R^2,\delta_1$	$1/R^3,\delta_1$	Index	$1/R,\delta_0$	$1/R^2,\delta_0$	$1/R^2,\delta_1$	$1/R^3,\delta_1$
1	0.00220234	0.00470252	0.00451061	0.04286517	22	0.11819686	0.11515361	0.11537466	0.01494637
2	0.00777611	0.02100319	0.02100594	0.05950544	23	0.11819686	0.11515361	0.11537466	0.01494637
3	0.00777611	0.02100319	0.02100594	0.05950544	24	0.11819686	0.11515361	0.11537466	0.01494637
4	0.00777611	0.02100319	0.02100594	0.05950544	25	0.11819686	0.11515361	0.11537466	0.01494637
5	0.00777611	0.02100319	0.02100594	0.05950544	26	0.11819686	0.11515361	0.11537466	0.01494637
6	0.00777611	0.02100319	0.02100594	0.05950544	27	0.11819686	0.11515361	0.11537466	0.01494637
7	0.00777611	0.02100319	0.02100594	0.05950544	28	0.07686574	0.12263703	0.12214112	0.39570127
8	0.00679017	0.01330923	0.01330666	0.02323701	29	0.43791324	1.14520979	1.14373494	3.18531361
9	0.00679017	0.01330923	0.01330666	0.02323701	30	0.26201938	0.35914198	0.35914157	0.53453506
10	0.00679017	0.01330923	0.01330666	0.02323701	31	0.26201938	0.35914198	0.35914157	0.53453506
11	0.00679017	0.01330923	0.01330666	0.02323701	32	0.26201938	0.35914198	0.35914157	0.53453506
12	0.00679017	0.01330923	0.01330666	0.02323701	33	0.26201938	0.35914198	0.35914157	0.53453506
13	0.00679017	0.01330923	0.01330666	0.02323701	34	0.26201938	0.35914198	0.35914157	0.53453506
14	0.00391254	0.00575585	0.00575901	0.01046399	35	0.26201938	0.35914198	0.35914157	0.53453506
15	0.51449689	3.52670107	2.82339324	19.18377655	36	0.17032050	0.13477474	0.13477469	0.08542104
16	0.20503061	0.45126803	0.45060429	1.18152861	37	0.17032050	0.13477474	0.13477469	0.08542104
17	0.20503061	0.45126803	0.45060429	1.18152861	38	0.17032050	0.13477474	0.13477469	0.08542104
18	0.20503061	0.45126803	0.45060429	1.18152861	39	0.17032050	0.13477474	0.13477469	0.08542104
19	0.20503061	0.45126803	0.45060429	1.18152861	40	0.17032050	0.13477474	0.13477469	0.08542104
20	0.20503061	0.45126803	0.45060429	1.18152861	41	0.17032050	0.13477474	0.13477469	0.08542104
21	0.20503061	0.45126803	0.45060429	1.18152861	42	0.10339405	0.08736277	0.08736257	0.12214912

The listed quadrature weights over the tensor product nodes are converted from the brute-force integration using $n=64$ so $N=524{,}288$. Refer to Section 5 for the meanings of brute-force quadrature parameters n and N.

Finally, the size δ of the exclusion volume V_δ is specified in the tables as either $\delta_0=0$ or $\delta_1=(5-\sqrt{15})/20$, which is the half of the smallest distance for the quadrature nodes to the boundary of the sphere.

Table 16: Weights for when the singularity is at $((5+\sqrt{15})/10,0,0)$. After a rotation, this table can be used when the singularity is at index 29 or 42: at the outer point on either line in Fig. 6. $\delta_0=0$ and $\delta_1=(5-\sqrt{15})/20$.

Index	$1/R,\delta_0$	$1/R^2,\delta_0$	$1/R^2,\delta_1$	$1/R^3,\delta_1$	Index	$1/R,\delta_0$	$1/R^2,\delta_0$	$1/R^2,\delta_1$	$1/R^3,\delta_1$
1	−0.00325314	−0.01928140	−0.02046529	−0.00786846	22	0.08559016	0.06584665	0.06584577	0.03809716
2	0.00293390	0.00157161	0.00156760	−0.00263126	23	0.08559016	0.06584665	0.06584577	0.03809716
3	0.00293390	0.00157161	0.00156760	−0.00263126	24	0.08559016	0.06584665	0.06584577	0.03809716
4	0.00293390	0.00157161	0.00156760	−0.00263126	25	0.08559016	0.06584665	0.06584577	0.03809716
5	0.00293390	0.00157161	0.00156760	−0.00263126	26	0.08559016	0.06584665	0.06584577	0.03809716
6	0.00293390	0.00157161	0.00156760	−0.00263126	27	0.08559016	0.06584665	0.06584577	0.03809716
7	0.00293390	0.00157161	0.00156760	−0.00263126	28	0.05287837	0.04684672	0.04684657	0.06997835
8	0.00382574	0.00483059	0.00483238	0.00669000	29	0.69602647	3.79125422	3.08221211	19.40373408
9	0.00382574	0.00483059	0.00483238	0.00669000	30	0.23497738	0.31533962	0.31512758	0.54626377
10	0.00382574	0.00483059	0.00483238	0.00669000	31	0.23497738	0.31533962	0.31512758	0.54626377
11	0.00382574	0.00483059	0.00483238	0.00669000	32	0.23497738	0.31533962	0.31512758	0.54626377
12	0.00382574	0.00483059	0.00483238	0.00669000	33	0.23497738	0.31533962	0.31512758	0.54626377
13	0.00382574	0.00483059	0.00483238	0.00669000	34	0.23497738	0.31533962	0.31512758	0.54626377
14	0.00232438	0.00134727	0.00134807	−0.00163993	35	0.23497738	0.31533962	0.31512758	0.54626377
15	0.24112607	0.65534847	0.65846090	1.70282726	36	0.13160204	0.06764054	0.06771117	−0.02646895
16	0.13395052	0.18457550	0.18457764	0.27746671	37	0.13160204	0.06764054	0.06771117	−0.02646895
17	0.13395052	0.18457550	0.18457764	0.27746671	38	0.13160204	0.06764054	0.06771117	−0.02646895
18	0.13395052	0.18457550	0.18457764	0.27746671	39	0.13160204	0.06764054	0.06771117	−0.02646895
19	0.13395052	0.18457550	0.18457764	0.27746671	40	0.13160204	0.06764054	0.06771117	−0.02646895
20	0.13395052	0.18457550	0.18457764	0.27746671	41	0.13160204	0.06764054	0.06771117	−0.02646895
21	0.13395052	0.18457550	0.18457764	0.27746671	42	0.08789093	0.09118974	0.09103143	0.21381388

Table 17: Weights for when the singularity is at $((5-\sqrt{15})/10,0,\pi/3)$. After a rotation, this table can be used when the singularity is at index 2 through 14: on either inner circle in Fig. 6. $\delta_0=0$ and $\delta_1=(5-\sqrt{15})/20$.

Index	$1/R,\delta_0$	$1/R^2,\delta_0$	$1/R^2,\delta_1$	$1/R^3,\delta_1$	Index	$1/R,\delta_0$	$1/R^2,\delta_0$	$1/R^2,\delta_1$	$1/R^3,\delta_1$
1	0.02580601	0.20872660	0.19510865	1.57336905	22	0.23165118	0.56443031	0.56444883	1.61141332
2	0.05571823	0.95055701	0.42144649	4.46641972	23	0.21161966	0.46225149	0.46226210	1.13307125
3	0.03647145	0.35650458	0.28107880	2.47757917	24	0.18098881	0.33011603	0.33011743	0.65248306
4	0.02195092	0.15096920	0.10710138	0.53987317	25	0.16803067	0.27722914	0.27722380	0.46590911
5	0.01447496	−0.04613472	0.05509650	−0.06192855	26	0.18098881	0.33011603	0.33011743	0.65248306
6	0.02195092	0.15096920	0.10710138	0.53987317	27	0.21161966	0.46225149	0.46226210	1.13307125
7	0.03647145	0.35650458	0.28107880	2.47757917	28	0.12827801	0.20465930	0.20465701	0.26485979
8	0.03266666	0.25988297	0.24185168	1.94186601	29	0.18630843	0.21635326	0.21634079	0.18712871
9	0.02582536	0.16312703	0.16042715	1.03481963	30	0.25809012	0.29492690	0.29667386	0.08562588
10	0.01853622	0.08908088	0.08692489	0.43074045	31	0.24590883	0.28151345	0.28166775	0.21469983
11	0.01565300	0.05902257	0.05921989	0.19316549	32	0.22337588	0.24037900	0.24056043	0.23290726
12	0.01853622	0.08908088	0.08692489	0.43074045	33	0.21318591	0.22302554	0.22267038	0.25256472
13	0.02582536	0.16312703	0.16042715	1.03481963	34	0.22337588	0.24037900	0.24056043	0.23290726
14	0.01077020	0.01818360	0.02544137	−0.14942952	35	0.24590883	0.28151345	0.28166775	0.21469983
15	0.17886367	0.44635454	0.44636981	1.29602187	36	0.24420721	0.28013190	0.28011579	0.24271125
16	0.26640590	0.79940098	0.79116425	3.11853716	37	0.23324973	0.26012477	0.26012041	0.25030599
17	0.23723474	0.60494413	0.60414444	1.87438837	38	0.21346861	0.22091537	0.22091362	0.21362004
18	0.19531172	0.38883105	0.38800375	0.85665455	39	0.20448804	0.20338749	0.20338900	0.19668758
19	0.17740445	0.29545149	0.29710985	0.38392198	40	0.21346861	0.22091537	0.22091362	0.21362004
20	0.19531172	0.38883105	0.38800375	0.85665455	41	0.23324973	0.26012477	0.26012041	0.25030599
21	0.23723474	0.60494413	0.60414444	1.87438837	42	0.15669647	0.15992724	0.15993242	0.17142351

Note that the weights are given for nodes in Cartesian coordinates. Since the weights contain the Jacobian for the transformation from spherical to Cartesian coordinates, convert the nodes to Cartesian coordinates according to the mapping

$$(\rho,\phi,\theta)\mapsto(\rho\cos(\phi)\sin(\theta),\rho\sin(\phi)\sin(\theta),\rho\cos(\theta)) \tag{D.1}$$

before using them with the tables of weights.

Table 18: Weights for when the singularity is at $(1/2,0,\pi/3)$. After a rotation, this table can be used when the singularity is at index 16 through 27: on either middle circle in Fig. 6. $\delta_0=0$ and $\delta_1=(5-\sqrt{15})/20$.

Index	$1/R,\delta_0$	$1/R^2,\delta_0$	$1/R^2,\delta_1$	$1/R^3,\delta_1$	Index	$1/R,\delta_0$	$1/R^2,\delta_0$	$1/R^2,\delta_1$	$1/R^3,\delta_1$
1	0.00609785	0.01789320	0.01789242	0.05477451	22	0.22553466	0.54046322	0.53947049	1.52974823
2	0.00478749	0.01064526	0.01049308	0.04847989	23	0.17058102	0.30127489	0.30114968	0.60075512
3	0.00747508	0.02157475	0.02155717	0.07058134	24	0.12083140	0.15564833	0.15552451	0.25878033
4	0.00684124	0.01357339	0.01355958	0.02439820	25	0.10069798	0.09216446	0.09216494	0.06890141
5	0.00722037	0.01530681	0.01533609	0.02850013	26	0.12083140	0.15564833	0.15552451	0.25878033
6	0.00684124	0.01357339	0.01355958	0.02439820	27	0.17058102	0.30127489	0.30114968	0.60075512
7	0.00747508	0.02157475	0.02155717	0.07058134	28	0.06422785	−0.00816267	−0.00774967	−0.31688628
8	0.00790165	0.02239892	0.02239785	0.06745562	29	0.22230357	0.33245721	0.33245628	0.52720844
9	0.00758641	0.01865117	0.01865103	0.04591909	30	0.44001342	1.01817588	1.01694809	2.68330840
10	0.00645011	0.01232327	0.01232305	0.02321762	31	0.30960480	0.51348859	0.51336413	0.95918778
11	0.00598800	0.01003304	0.01003319	0.01512090	32	0.19449144	0.20353347	0.20341144	0.27922689
12	0.00645011	0.01232327	0.01232305	0.02321762	33	0.14179475	0.03159335	0.03183850	−0.26322292
13	0.00758641	0.01865117	0.01865103	0.04591909	34	0.19449144	0.20353347	0.20341144	0.27922689
14	0.00481037	0.00780829	0.00780867	0.00721579	35	0.30960480	0.51348859	0.51336413	0.95918778
15	0.17819955	0.43299242	0.43224764	1.21426996	36	0.28227223	0.41321066	0.41320942	0.65347429
16	0.47990829	2.98081056	2.39502028	15.88986922	37	0.22803542	0.26765494	0.26765478	0.33356589
17	0.26489067	0.86005135	0.80022922	3.30071380	38	0.16872588	0.14685038	0.14685022	0.14169025
18	0.14830022	0.35327182	0.29521258	1.34635389	39	0.14529757	0.09960350	0.09960352	0.06133652
19	0.07295410	−0.33088962	−0.21397437	−2.64077459	40	0.16872588	0.14685038	0.14685022	0.14169025
20	0.14830022	0.35327182	0.29521258	1.34635389	41	0.22803542	0.26765494	0.26765478	0.33356589
21	0.26489067	0.86005135	0.80022922	3.30071380	42	0.10194945	0.03797657	0.03797708	−0.06224900

Table 19: Weights for when the singularity is at $((5+\sqrt{15})/10,0,\pi/3)$. After a rotation, this table can be used when the singularity is at index 30 through 41: on either outer circle in Fig. 6. $\delta_0=0$ and $\delta_1=(5-\sqrt{15})/20$.

Index	$1/R,\delta_0$	$1/R^2,\delta_0$	$1/R^2,\delta_1$	$1/R^3,\delta_1$	Index	$1/R,\delta_0$	$1/R^2,\delta_0$	$1/R^2,\delta_1$	$1/R^3,\delta_1$
1	0.00190925	0.00021662	0.00021630	−0.00464157	22	0.14483430	0.21391864	0.21391946	0.34271845
2	−0.00115379	−0.01363555	−0.01463125	−0.00202242	23	0.11569392	0.13503317	0.13503327	0.16761500
3	0.00196273	−0.00215062	−0.00225074	−0.00911233	24	0.08533163	0.07414691	0.07414701	0.07255990
4	0.00362742	0.00407500	0.00397566	0.00904608	25	0.07322515	0.04967017	0.04967017	0.03038798
5	0.00435265	0.00676153	0.00696056	0.00325564	26	0.08533163	0.07414691	0.07414701	0.07255990
6	0.00362742	0.00407500	0.00397566	0.00904608	27	0.11569392	0.13503317	0.13503327	0.16761500
7	0.00196273	−0.00215062	−0.00225074	−0.00911233	28	0.05059697	0.01599882	0.01599848	−0.03874150
8	0.00266135	0.00049618	0.00049574	−0.00584562	29	0.20530332	0.30616554	0.30592752	0.57077436
9	0.00341690	0.00341011	0.00341008	0.00276241	30	0.63634852	3.17847009	2.58769746	16.09155068
10	0.00357507	0.00375086	0.00375080	0.00341027	31	0.31492701	0.72233774	0.66286296	2.43901973
11	0.00358178	0.00393717	0.00393718	0.00425699	32	0.17382416	0.33825205	0.27934127	1.44333039
12	0.00357507	0.00375086	0.00375080	0.00341027	33	0.06383385	−0.45662412	−0.33854721	−2.98066335
13	0.00341690	0.00341011	0.00341008	0.00276241	34	0.17382416	0.33825205	0.27934127	1.44333039
14	0.00310721	0.00452523	0.00452541	0.00762016	35	0.31492701	0.72233774	0.66286296	2.43901973
15	0.11407893	0.17184068	0.17184129	0.27543937	36	0.25981578	0.38322787	0.38291055	0.72517750
16	0.23843004	0.57603175	0.57862912	1.42724339	37	0.19327321	0.20150759	0.20146781	0.24944161
17	0.16068718	0.27253469	0.27279542	0.50909091	38	0.13597065	0.10307084	0.10303120	0.11242237
18	0.09890559	0.10483550	0.10509483	0.13785636	39	0.11247389	0.05768264	0.05768270	0.02198106
19	0.06885575	0.00417790	0.00365860	−0.14509165	40	0.13597065	0.10307084	0.10303120	0.11242237
20	0.09890559	0.10483550	0.10509483	0.13785636	41	0.19327321	0.20150759	0.20146781	0.24944161
21	0.16068718	0.27253469	0.27279542	0.50909091	42	0.06962562	−0.01893673	−0.01880458	−0.18093511

References

[1] D. Chen, W. Cai, B. Zinser, and M. Cho. Accurate and Efficient Nyström Volume Integral Equation Method for the Maxwell equations for Multiple 3-D Scatterers. Journal of Computational Physics, 321 (2016), 303-320.

[2] M.S. Tong and Weng Cho Chew. Super-hyper singularity treatment for solving 3D electric field integral equations. Microwave and Optical Technology Letters, 49.6 (2007), 1383-1388.

[3] J. Shen. Efficient spectral-Galerkin methods IV. Spherical geometries. SIAM J. Sci. Comput., 20 (1999), 1438-1455.

[4] J. Boyd. Chebyshev and Fourier Spectral Methods. Dover, Mineola, 2001.

[5] Wolfram Research, Inc., Mathematica, Version 10.0, Champaign, IL (2014).